JOURNAL OF EXPERIMENTAL ZOOLOGY (MOL DEV EVOL) 291:30–57 (2001)

Theory of the Growth and Evolution of Feather Shape

RICHARD O. PRUM* AND SCOTT WILLIAMSON
Department of Ecology and Evolutionary Biology, and Natural History Museum, University of Kansas, Lawrence, Kansas 66045

ABSTRACT We present the first explicit theory of the growth of feather shape, defined as the outline of a pennaceous feather vane. Based on a reanalysis of data from the literature, we propose that the *absolute* growth rate of the barbs and rachis ridges, not the vertical growth rate, is uniform throughout the follicle. The growth of feathers is simulated with a mathematical model based on six growth parameters: (1) absolute barb and rachis ridge growth rate, (2) angle of helical growth of barb ridges, (3) initial barb ridge number, (4) new barb ridge addition rate, (5) barb ridge diameter, and (6) the angle of barb ramus expansion following emergence from the sheath. The model simulates growth by cell division in the follicle collar and, except for the sixth parameter, does not account for growth by differentiation in cell size and shape during later keratinization. The model can simulate a diversity of feather shapes that correspond closely in shape to real feathers, including various contour feathers, asymmetrical feathers, and even emarginate primaries. Simulations of feather growth under different parameter values demonstrate that each parameter can have substantial, independent effects on feather shape. Many parameters also have complex and redundant effects on feather shape through their influence on the diameter of the follicle, the barb ridge fusion rate, and the internodal distance. Simulated isochrones—the loci, or sets, of feather cells of the same age—have the same oblique chevron-shaped position in the mature feather as fault bars, which are isochronic defects in the barbules created by a disruptions during development. Accurate simulation of fault bar shape and position confirms the uniform absolute growth rate hypothesis and the general realism of the model. The theory defines a six-parameter feather morphospace, and provides many predictions about the developmental determination of feather shape that can be tested with detailed observations and experiments on developing feathers. This theory also provides testable predictions about the changes in developmental mechanisms required to evolve different feather shapes to accomplish various functions. *J. Exp. Zool. (Mol. Dev. Evol.) 291:30–57, 2001.*

A basic principle of developmental biology is that complex shapes and spatial patterns are not specified in precise detail (Thompson, ’42; Ball, ’98). Rather, complex forms are created by fundamental physical, chemical, and cellular interactions whose precise outcome is specified by relatively few critical parameters. Thus, the growth of many diverse biological forms can be understood in terms of similar general developmental models and basic parameters (Thompson, ’42; Ball, ’98). However, some biological forms grow by such distinct mechanisms that they require unique explanatory models that incorporate specific parameters. For example, the diversity in shape of mollusk shells can be described by a unique developmental model based on the shape of the growing surface, the growth in size of the growing surface, and the angle of its rotation during growth around an axis (Raup and Michelson, ’65). The evolution of molluscan diversity involved the exploration of this potential shell morphospace.

Feathers are extraordinarily diverse and complex structures. Feathers are the most complex epidermal appendages found in animals (Lucas and Stettenheim, ’72). They are uniquely characterized by their complex branched structure and striking diversity in size, shape, color, and texture (Lucas and Stettenheim, ’72; Brush, ’93, ’96; Prum, ’99). Feathers are branched like plants, but, unlike typical plants, feathers do not grow from bifurcating shoots. Rather, feathers grow from their bases like hairs. Feathers grow from a

*Correspondence to: Richard O. Prum, Natural History Museum, Dyche Hall, University of Kansas, Lawrence, KS 66045-2454.
E-mail: prum@ukans.edu
Received 31 March 2000; Accepted 27 October 2000

unique organ—the feather follicle—which is characterized by a cylindrical invagination of a epidermal tissue (Lucas and Stettenheim, '72; Prum, '99). Feather follicles have evolved a unique developmental mechanism—the helical growth of barb ridges—in order to grow a branched epidermal appendage from its base (Lucas and Stettenheim, '72; Prum, '99). Feathers are amazingly diverse in shape, and they range over five orders of magnitude in size from less than 1 mm to over 10 m in certain captive-bred fowl (Young, '99). Feathers can function in flight, swimming, thermoregulation, physical protection, visual and tactile communication, sound production, tactile and auditory sensation, foraging, water repellency, and even water transport (Stettenheim, '76). A preliminary conceptual model of the evolution of this morphological and functional diversity requires an explicit developmental theory of the mechanisms by which feather shape is determined.

The growth and evolution of feather shape diversity have so far eluded any general theory or explicit modeling. The growth of different feather shapes must be understood in terms of the developmental mechanisms operating within the follicle collar—the layer of cells at the base of the internal epidermal layer of the tubular feather follicle. The anatomical details of feather growth have been well described (Davies, 1889; Strong, '02; Greite, '34; Hosker, '36; 'Espinasse, '39; Lucas and Stettenheim, '72), and a new generation of studies is beginning to examine the molecular basis of many features of feather development (e.g., Chuong et al., '90; Chuong, '93; Nohno et al., '95; Ting-Berreth and Chuong, '96a, b; Chuong and Widelitz, '98). However, little research has been done explicitly on the growth of feather shape (Lucas and Stettenheim, '72; Spearman, '73; Sawyer et al., '86; Edelman, '88; Brush, '93, '96).

We have found only a few previous hypotheses in the literature about the effect of cell growth in the follicle collar on feather shape. Lillie and Juhn ('32) proposed that differential growth rates among barb ridges of the follicle produced the variations in feather shape and symmetry. This hypothesis was quickly falsified ('Espinasse, '34, '39; Hosker, '36), but has remained surprisingly influential (e.g., Lucas and Stettenheim, '72: 371). Subsequently, 'Espinasse ('39: 281) hypothesized that the shape of the feather vane "is clearly determined by (a) the length of the barbs and (b) the angle they take up, when dry, with the rachis." 'Espinasse was correct to reject differential barb ridge growth rates, but his model of feather shape determination was simplistic and incomplete. In their exhaustive survey of the morphology and development of feathers, Lucas and Stettenheim ('72: 371) wrote only that, "Variations in the rates at which [barb] ridges form and grow affect the final lengths of the barbs and hence the shape of the vanes." This brief statement incorporated the erroneous differential barb ridge growth rate hypothesis of Lillie and Juhn ('32), but it explicitly hypothesized for the first time that the rate of new barb ridge addition is a critical determinant of feather shape. Some authors have noted the role of deciduous barbs in the producing the racket-tipped rectrices of motmots (Motmotidae; Beebe, '10; Wagner, '59; Bleiweiss, '87), but these feather shape changes occur after feather growth is completed. Bleiweiss ('87) described the morphology of barbs and barbules in a diversity of racket-shaped feathers that lack deciduous barbs, and are thus determined by follicular growth mechanisms. Bleiweiss ('87) proposed that the reduced barb lengths that create the constrictions in vane width characteristic of these racket-shaped feathers are a consequence of the position in the follicle at which new barb ridges are added, and their angle of growth toward the dorsal margin. Bleiweiss ('87) correctly identified the role of the angle of helical growth of barb ridges in the growth of feather shape. However, the hypothesis that barb length is controlled by the position of new barb ridge addition in the follicle is based on the inaccurate notion that the follicle has a fixed diameter that that can sometimes be greater in size than the barb and rachis ridges it contains (Bleiweiss, '87). Histological cross-sections of growing feathers document that follicle diameter is determined by the barb and rachis ridges it contains, and that new barb ridge addition takes place at a single posterior new barb locus, or, if there is an aftershaft, at two laterally displaced new barb loci (e.g., Strong, '02; Hosker, '36; 'Espinasse, '39; Lucas and Stettenheim, '72).

Currently, there is no generalized theory or explicit model of the determination of the feather shape based on the known mechanisms of development in the feather follicle. Fortunately, the relationship between developmental mechanisms of the follicle and feather shape is amenable to mathematical modeling. In this article, we review the basic details of feather morphology and growth. Next, we discuss the previous literature on feather barb and rachis ridge growth rates, an understanding of which is critical to creating a realistic theory of feather shape determination. Based on

our reanalysis of this literature, we propose that the *absolute* growth rate of the barb and rachis ridges, independent of direction, is uniform throughout the follicle collar. We then present a six-parameter mathematical model of the growth of pennaceous feathers that is based on known mechanisms of development in the feather follicle. We use the model to document the independent effects of these parameters on the development of feather shape, to explore the diversity of possible feather shapes, and to model the position of isochronic feather fault bars. We compare the results of these simulations to known feather morphologies, summarize the complex developmental dynamics among the parameters in the model, and confirm the hypothesis that the absolute growth rate of the barb and rachis ridges is uniform throughout the follicle. Last, we propose several tests of this theory that can be conducted using detailed observations and experimental manipulations of feathers, and discuss the implications of the model for the study of the evolution of feather shape.

FEATHER MORPHOLOGY

A feather is a branched, or pinnate, epidermal derivative composed of a matrix of keratin (Fig. 1A; feather morphology is thoroughly reviewed in Lucas and Stettenheim, '72). A typical contour feather is composed of the calamus that extends into the rachis, the central shaft of the feather vane. The primary branches of the rachis are the barbs. The shaft of a barb is called the ramus. The rami support the secondary branches of the feather, which are called barbules (Fig 1A, B). The barbules oriented away from and toward the base of the feather are referred to as the distal and proximal barbules, respectively. The structural and functional diversity of feathers is a consequence of microstructural variation in the form of the rachis, rami, and barbules. The closed, planar vane of a pennaceous feather is created by the interlocking interaction of the hooked tips, or pennulae, of the distal barbules and the simpler, grooved bases of the proximal barbules of neighboring barbs (Fig. 1B) (Dyck, '85). In contrast, plumulaceous feathers, or downs, lack hooked pennulae, and have elongate barbules with nodal prongs that form disorderly tangles. Contour feathers of many birds have an afterfeather—a second, usually smaller and plumulaceous feather grown from the same follicle (Fig. 1A).

FEATHER GROWTH

Feathers are essentially cylindrical structures that grow from the base of the inner layer of the cylindrical feather follicle—called the collar (feather growth is thoroughly reviewed in Lucas and Stettenheim, '72; Prum, '99). Most of the follicles that produce all the feathers in a bird's life develop during the first 12 days of life in the egg (Lucas and Stettenheim, '72). First, an epidermal placode that specifies the location of the feather follicle appears (Fig. 2A). Proliferation of dermal cells under the placode produces a finger-like feather papilla, or feather bud (Fig. 2B). The papilla quickly establishes an anterior–posterior orientation that remains fixed throughout the life of the bird. Next, the epidermis proliferates around the base of the papilla creating a cylindrical invagination into the dermis around the base of the papilla (Fig. 2C). The outer epidermal layer forms the walls of the socket of the feather follicle, whereas the inner epidermal layer becomes the collar (Fig. 2D).

Virtually all cell division during feather growth takes place in the collar (also called the ramogenic zone; Lucas and Stettenheim, '72). Growth proceeds by proliferation of the keratinocytes, which produce feather keratin. As younger cells proliferate basally, older keratinocytes are displaced upward and out of the collar. The dermal pulp at the center of the follicle supplies nutrients for the growth of the feather, and is also the source of feather pigments. As the keratinocytes are displaced upward, they begin to produce intracellular keratin. Eventually, the keratinocytes become isolated from nutrients provided by the dermal pulp, and they die leaving behind the deposited keratin matrix that constitutes the mature feather.

The distinct feather filaments—the barbs, barbules, and rachis—are created by differentiation and morphogenesis within the follicle collar (Figs. 2D, 3). The outer layer of the collar produces a thin cylinder of keratin, which forms the superficial, deciduous sheath of the emerging feather (Fig. 3.1). The intermediate layer of the collar becomes organized into a series of longitudinal ridges known as barb ridges (Fig. 3.1). Proliferation of keratinocytes within the differentiated barb ridges produces the filaments that become the rachis, barbs, and barbules of the growing feather.

The primary branched structure of a pinnate feather is produced by the helical displacement of barb ridges toward the anterior midline of the follicle as they grow (Figs. 3.3, 4). Within each barb ridge, new cells do not grow directly below the older, more superficial cells. Rather, each successive layer of cells is displaced in position within the cylindrical collar toward the anterior midline

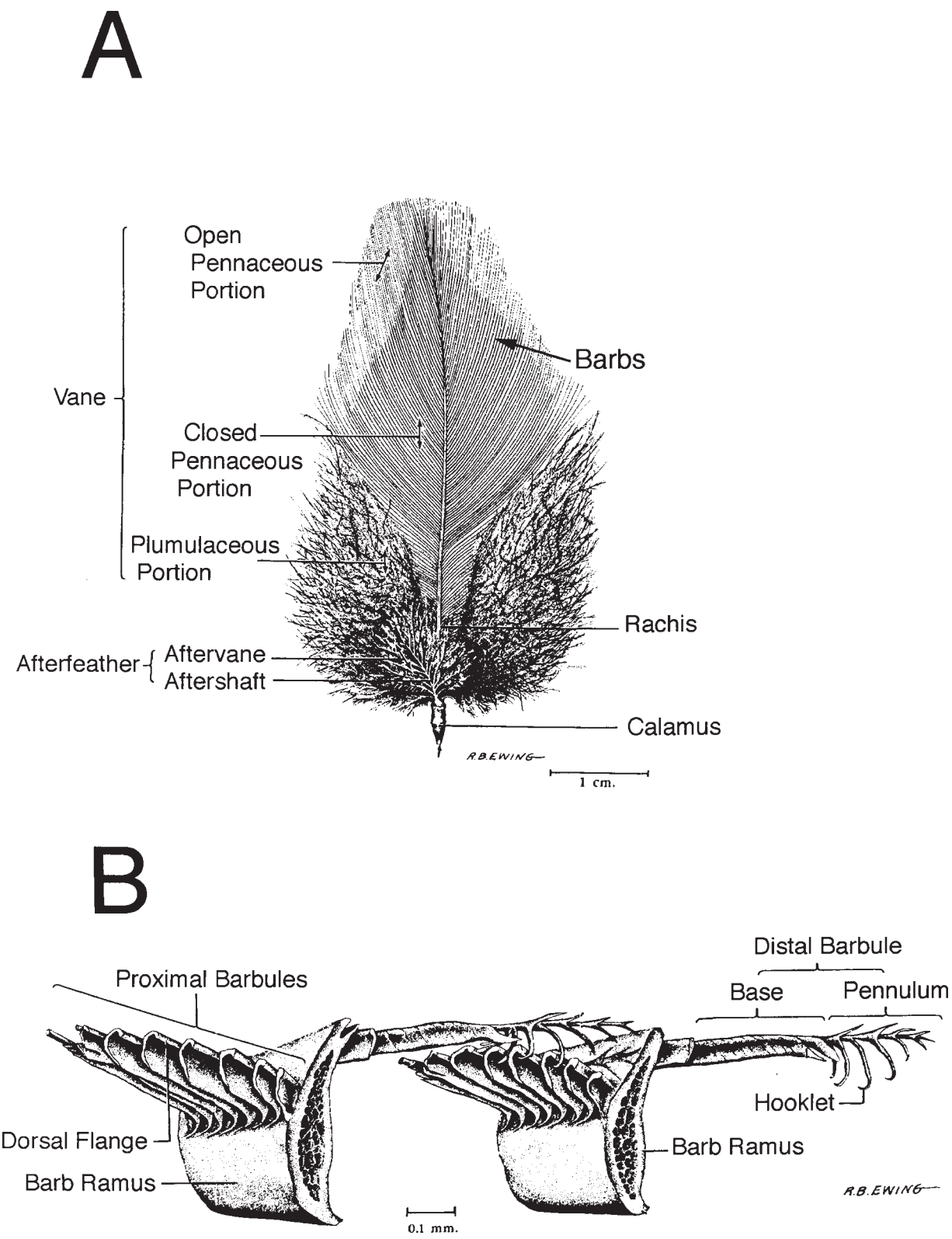

Fig. 1. (**A**) The structure of a typical pennaceous contour feather with afterfeather. (**B**) Cross-section of two feather barbs from the closed pennaceous portion of a feather vane (orientation as in the labeled Barbs in A) showing the differentiation between the distal barbules (oriented toward the tip of the feather) and the proximal barbules (oriented toward the base of the feather). The hooked pennulae of the distal ends of the distal barbules extend over the obverse (upper) surface of the vane to interlock with the grooved dorsal flanges of the bases of the proximal barbules from the adjacent barbs to form the closed pennaceous vane. The distal barbules of open pennaceous feathers lack hooked pennulae. Both illustrations from Lucas & Stettenheim ('72).

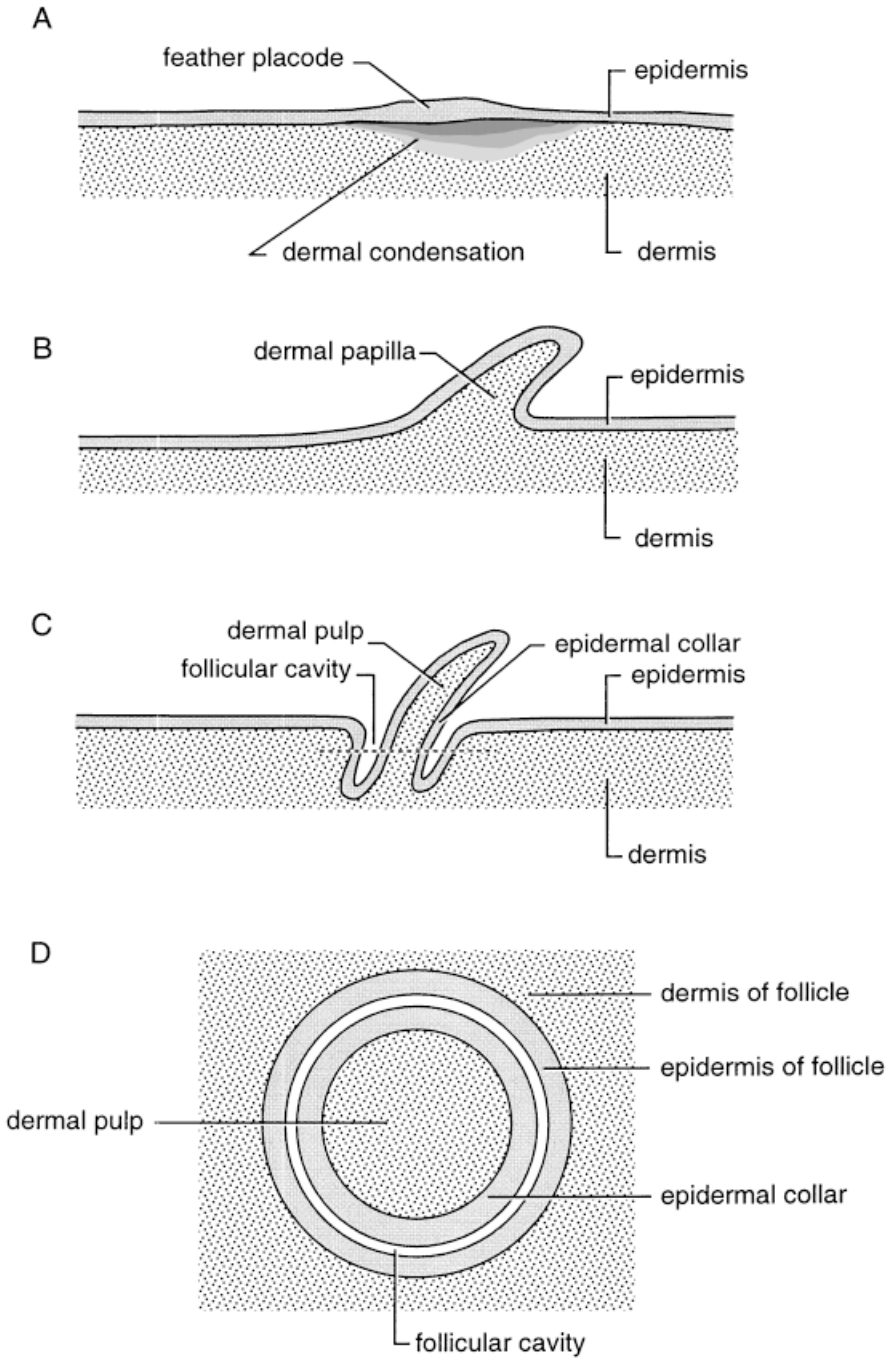

Fig. 2. Schematic diagram of the development of a feather follicle. (**A**) Development of the epidermal feather placode and the dermal condensation. (**B**) Development of a feather papilla through the proliferation of dermal cells. (**C**). Formation of the feather follicle through the invagination of a cylinder of epidermal tissue around the base of the feather papilla. (**D**) Cross-section of the feather follicle through the horizontal plane indicated by the dotted line in C. The follicle is characterized by the juxtaposition of a series of tissue layers (from peripheral to central): the dermis of the follicle, the epidermis of the follicle (outer epidermal layer), the follicle cavity or lumen (the space between epidermal layers), the follicle collar (inner epidermal layer or ramogenic zone), and the dermal pulp (tissue at the center of the follicle). The proliferation of feather keratinocytes takes place in the follicle collar, the inner epidermal layer.

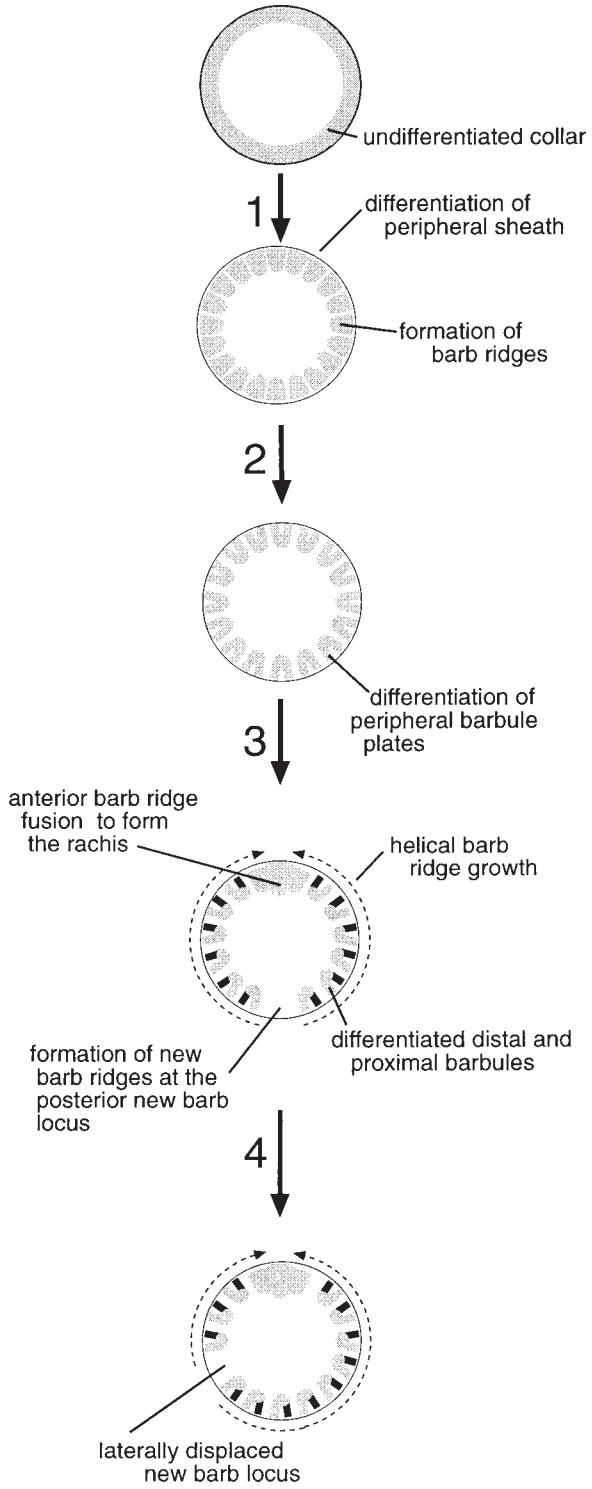

Fig. 3. Diagram of feather development depicted as a series of cross-sections of the follicle collar (See 2D). (Top) The collar begins as an undifferentiated tubular tissue. (1) The collar differentiates into a peripheral sheath and longitudinal barb ridges. (2) The barb ridges differentiate into the peripheral barbule plates and the ramus. (3) The barb ridges begin grow helically around the circumference of the follicle toward the anterior midline where they fuse to form the rachis ridge. When the reach the anterior midline, subsequent barb ridges fuse to the rachis ridge. New barb ridges are formed at the posterior new barb locus and begin helical growth from a posterior position. The distal and proximal barbule plates differentiate to form the hooked and grooved barbules that produce the closed pennaceous vane. (4) In asymmetrical feathers, differential barb ridge addition displaces the new barb locus laterally and produces a asymmetrical vane.

of the follicle (Lucas and Stettenheim, '72). As the first barb ridges reach the anterior midline of the follicle, they fuse to form the rachis ridge which becomes the feather rachis (Lucas and Stettenheim, '72). When they reach the rachis ridge, subsequent barb ridges fuse to it and are then finished growing. After fusion to the rachis, barbs are displaced upward and out of the follicle as the rachis grows. Meanwhile, new barb ridges form at the new barb locus at the posterior midline of the collar opposite the rachis ridge (Figs. 3.3, 4). These new barb ridges begin their helical growth around the collar from the posterior new barb locus to fuse with the rachis ridge anteriorly, creating the barbs of the left and right sides of the feather vane. As barb ridges are formed and fuse to the rachis, the follicle varies in diameter. As the feather approaches its final size, new barb ridges cease to form at the new barb locus, the follicle decreases in diameter, and the last barb ridges fuse to the rachis ridge. Ultimately, the collar resumes its undifferentiated cylindrical state forming the tubular calamus of the feather. The afterfeather (Fig. 1A) develops by the same general mechanism as the main vane; the new barb locus divides into two, and posterior barb ridges begin helical growth toward the posterior midline to form a second rachis and vane (Fig. 4).

The secondary feather branches—the barbules—are produced by differentiation within horizontal layers of the peripheral cells of the barb ridges (Fig. 3.2). The inner (or basilar) cells within the barb ridges form the ramus while the peripheral cells differentiate into the barbule plates that form the barbules of that barb. Each horizontal layer of cells constitutes a single barbule plate and becomes a single pair of barbules. First, the barbule plate differentiates into a lateral pair of plates by the death of the cells along its central axis. Then, the peripheral cells in the paired barbule plates become the distal cells of the barbules, and the more central cells become the base of the barbules that are fused to the ramus. [The development of barbule branching is a completely distinct mechanism from the development of barb branching, *contra* Edelman ('88) and others].

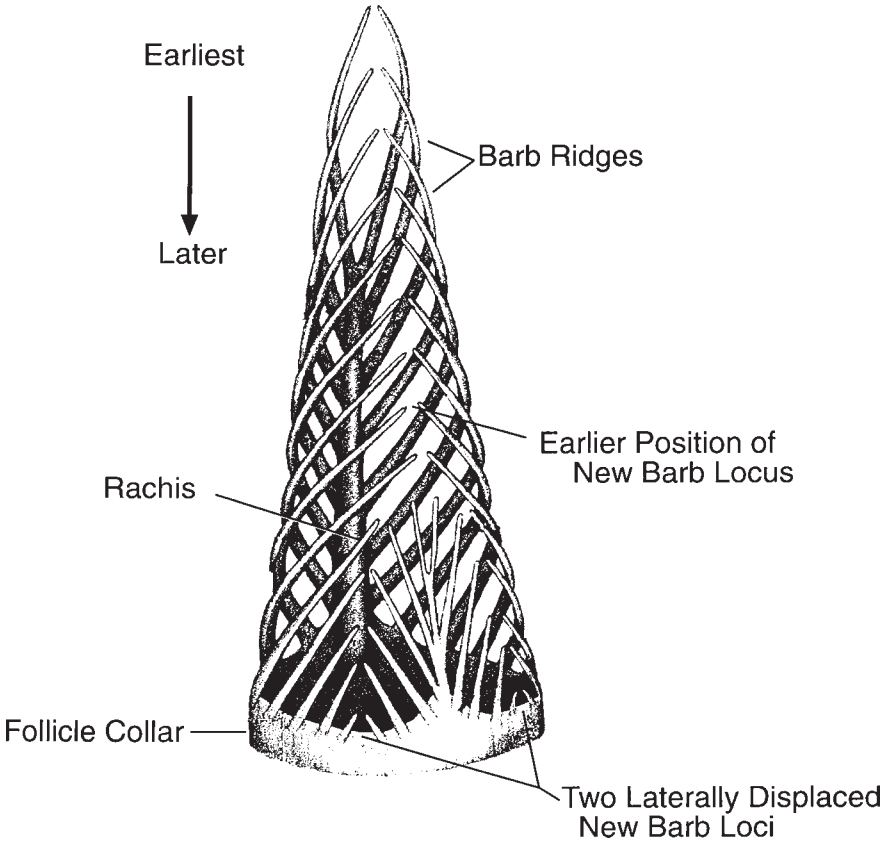

Fig. 4. Schematic diagram of helical growth of barb ridges within the follicle of a feather with a main feather and an afterfeather from Lucas and Stettenheim ('72). Initially, barb ridges form at the new barb locus on the posterior midline of the collar and grow helically around the collar toward the anterior midline where they fuse to the rachis ridge to form the rachis. In feathers with an afterfeather, the new barb locus divides into two laterally displaced new barb loci. Then new barb ridges are helically displaced anteriorly toward the main rachis and posteriorly to form the rachis and vane of the afterfeather. A mature contour feather with afterfeather is illustrated in Figure 1A.

The completed, emerging feather is a cylindrical structure of branched keratin filaments that is covered by a superficial, deciduous keratin sheath, and is commonly called a pin feather. As the cylindrical feather emerges from its sheath, the barb ridges expand to create the mature planar, pennaceous form of the final feather. The outer or peripheral surface of a cylindrical pin feather becomes the obverse ("dorsal") surface of the fully emerged pennaceous feather, whereas the basilar surface of the collar becomes the reverse ("ventral") surface of the feather vane (e.g., Greite, '34). Thus, the obverse and reverse surfaces of a feather are not homologous with anterior and posterior surfaces of a scale because the anterior and posterior surfaces of a scale develop from the anterior and posterior surfaces of the scale papilla, whereas the obverse and reverse surfaces of a feather come from the peripheral and basilar surfaces of the cylindrical follicle collar, respectively.

Each follicle produces a series of feathers during the life of the bird. The first feathers to emerge from most follicles are plumulaceous natal downs. Most of these same follicles will produce pennaceous contour feathers in subsequent molts. Thus, the diversity in shape and structure of feathers is not a consequence of variation in the structure of follicles but of the detailed specification of developmental parameters affecting feather shape and structure that are within the capacity of all follicles.

BARB RIDGE GROWTH RATES AND FEATHER SHAPE

Understanding the rate of barb ridge and rachis ridge growth in the collar is critical to constructing a realistic model of the growth of feather shape. Unfortunately, the literature on this subject has been confusing and this question remains unresolved.

The first analysis of barb ridge growth rates was conducted by Lillie and Juhn ('32) in an investigation of the response of the pigmentation of developing feathers to exposure to different dosages and durations of estrogen and thyroxin. Lillie and Juhn ('32) hypothesized that barb ridges grow most rapidly early in their development on the posterior side of the follicle, and that barb ridge growth rate decreases fivefold as they grow helically toward the anterior midline of the follicle to fuse to the rachis. They further hypothesized that variations in these growth rates among barb ridges of the posterior, anterior, left, and right sides of the follicle were responsible for determining feather shape and asymmetry. 'Espinasse ('34, '39) and Hosker ('36) cogently proved this hypothesis to be false, and provided evidence that barb ridge growth rates are uniform throughout the follicle at a given time. However, the hypothesis that variations in barb ridge growth rate determine feather shape continued to be cited (e.g., Lucas and Stettenheim, '72: 371), and confusion has remained about the relative growth rate of the barb and rachis ridges.

The consequences of uniform growth rates and helical growth can best be understood using the concept of an isochrone—the locus, or set, of cells in the feather that were formed at the same time within the follicle collar. Hardesty ('33) first defined the feather isochrone and hypothesized that an isochronic section of a feather vane is a line of cells "approximately at right angles to the rachis," a position that should occur if the vertical growth rates of the barbs and rachis are uniform. In a series of arcane papers, Juhn and Fraps ('36; Fraps and Juhn, '36a,b) analyzed the relationship between barb growth and the position of a feather isochrone by mounting feathers with all barbs placed at right angles to the rachis. They then hypothesized that in this configuration an isochrone includes all points along any line at a 45° angle to the rachis (i.e., the locus of cells that are the same linear distance on both the barbs and rachis from the points of fusion between that barb and the rachis). In a normal feather vane, this hypothesized isochronic line is not perpendicular to the rachis, but inclined slightly at the margins of the vane toward the base of the feather in an oblique chevron (Fraps and Juhn, '36a) (Fig. 5, T_6). Fraps and Juhn ('36a) compared the position of these hypothesized isochrones to the position of fault bars—defects in the morphology of the barbules of neighboring barbs that are caused by short-term disruptions of the feather during development (e.g., mechanical damage from handling or acute dietary deficiency). Indeed, fault bars are isochronic developmental abnormalities, and they are not perpendicular to the rachis but form a line inclined slightly toward the base of the feather at its margin in the same position as the isochrones hypothesized by Fraps and Juhn ('36a). Fraps and Juhn ('36a) concluded correctly that these data demonstrate that growth rates of the barb and rachis ridges are uniform, but they consistently stated in this and subsequent papers (Lillie and Juhn, '38; Lillie, '40 '42; Lillie and Wang, '40, '41) that it is the *axial* growth rates—the vertical growth along the central axis of the follicle—that are uniform. This conclusion was repeated by Lucas and Stettenheim ('72).

'Espinasse ('39) agreed with Fraps and Juhn ('36a) that a fault bar is an isochronic section of a feather vane, but he hypothesized that fault bars are perpendicular to the barb rami. 'Espinasse further hypothesized that the distortion in shape between the originally horizontal position of an isochrone within the collar and its ultimately oblique position in the emergent feather is due to the angle of barb ridge expansion during the unfurling of the vane from its original cylindrical shape.

Fraps's and Juhn's ('36a; Lillie and Juhn, '38; Lillie, '40 '42; Lillie and Wang, '40, '41) interpretation that *axial* growth of the barb and rachis ridges are uniform is incorrect. Fraps's and Juhn's data actually demonstrate that the isochronic points on feather barbs are the same *absolute* distance from the isochronic point on the rachis. Thus, it is the *absolute* growth rate—the absolute increase in length of the barb ridges and the rachis ridge per unit time independent of direction—that is uniform throughout the follicle, not the *axial* or vertical growth rate. The initial distortion in shape of an isochrone from horizontal at its origin in the collar to an oblique chevron in the developed feather, occurs because the barb and rachis ridges grow at the same absolute rate but in different directions (Fig. 5). Since the barb ridges grow helically around the collar, the same absolute increase in length over time will not produce the same vertical component of growth in the barbs as in the rachis, which grows directly vertically out of the follicle (Fig.6). Thus, the vertical growth rate of the rachis ridge and the barb ridges differ in relation to the angle of the helical growth of barb ridges around the follicle and the horizontal component of growth (Fig. 6; see Parameters).

Although the appropriate data have been avail-

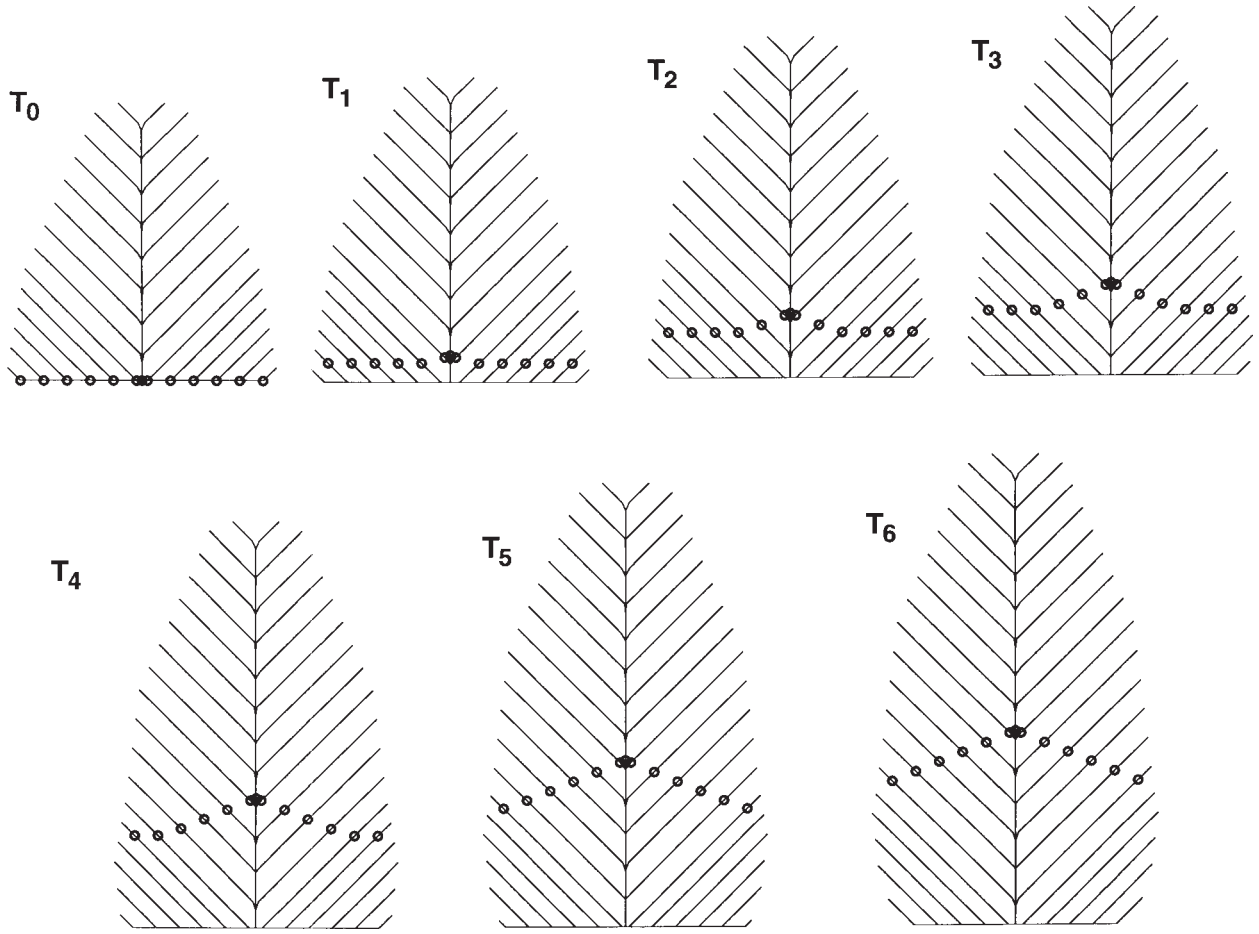

Fig. 5. The simulated spatiotemporal relationships among barb and rachis cells from an isochronic section of the follicle collar during feather development depicted at seven time stages (T_0–T_6). An isochrone is the locus or set of feather cells of the same age. The cylindrical collar is depicted as a horizontal line that has been divided down at posterior midline and flattened—anterior is central and posterior divided at the left and right sides. Growth in barb and rachis ridges is from the base. The isochronous cells (open circles) originate at the same time by cell division in the follicle collar (T_0). In subsequent time intervals (T_1–T_6), all barb and rachis ridges grow at the same absolute growth rate, *m*—the absolute increase in length per unit time independent of direction. The rachis ridge (the central vertical line) grows vertically at rate *m,* and the barb ridges grow helically around the follicle toward the rachis at rate *m*. Although the rachis and barb ridges grow at the same absolute rate, the isochronic rachis and barb cells grow vertically at different rates until the barb ridges are fused to the rachis. Then each barb ridge ceases growth and is displaced vertically at rate *m* with the rachis.

able since Fraps and Juhn ('36a), we do not know of any previous explicit statement of this fundamental detail of feather growth. Although diel, or daily, variations in feather growth rate are well documented (Lucas and Stettenheim, '72), these variations should affect all barb and rachis ridges equivalently. Thus, we propose that the absolute growth rate due to cell division in the follicle collar is uniform among all barb and rachis ridges despite any variations in that rate over time.

THE MODEL

Feather growth parameters

The model is structured around three basic assumptions: (1) Growth is from the bottom, occurring through cell division in a narrow band of cells around the base of the follicle. (2) The absolute growth rate is uniform for all barb ridges and the rachis ridge and is constant throughout feather growth. (3) The barb ridges are physically adjacent to each other, their diameters combine to determine the diameter of the follicle, and they cannot change their order within the collar.

We have identified and incorporated into our model five developmental parameters that are hypothesized to determine of the growth of feather shape during cell division in the feather follicle: (1) the absolute growth rate, (2) the angle of helical growth of barb ridges, (3) the initial number of barb ridges, (4) the new barb ridge addition rate

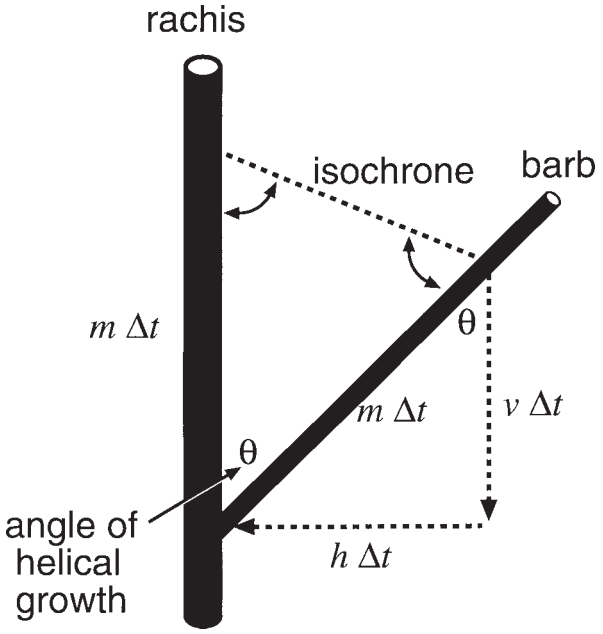

Fig. 6. Diagram of the relationship between the absolute growth rate, m, and the vertical, v, and horizontal, h, components of growth for the rachis ridge (vertical cylinder) and a single barb ridge (angled cylinder) with constant diameters. The barb ridge grows helically around the follicle at rate m and angle θ, but the vertical component of barb ridge growth, v, is given by $m\cos(\theta)$, and its horizontal component, h, is given by $m\sin(\theta)$. The rachis grows vertically ($\theta = 0$) at rate m, so $v = m$ and $h = 0$. An isochronic section connecting rachis and barb cells of the same age (dotted line) forms an isosceles triangle with the rachis and the barb. The two sides of equal length are given by $m\ \Delta t$—the growth rate times the time since common origin. The angles of the isochrone to the rachis and the barbs (curved double-headed arrows) are both $(180 - \theta)/2$.

over time, (5) the growth of barb ridge diameter (Fig. 7). An additional sixth parameter, (6) the angle of barb expansion (which occurs when growth is completed and after emergence from the sheath), is also included in the model (Fig. 7). Differential growth in cell size and cell shape also influences the ultimate feather shape after cell division within the follicle collar, but these variables are not included in this model because of the additional computational complexity.

Absolute growth rate

The absolute growth rate, m, is defined as the increase in length of the barb ridges or rachis ridge per unit time independent of the direction of growth (Fig. 6, 7). As discussed above, the absolute growth rate of barb ridges and the rachis ridge of a feather is uniform throughout the follicle. In our simulations, this parameter is also assumed to be constant in time throughout feather growth.

Angle of helical growth

The absolute growth of each barb ridge can be decomposed into horizontal and vertical components (Fig. 6, 7). For the rachis, the vertical component of growth is equal to the absolute growth rate because the rachis is growing vertically out of the follicle. The vertical component of barb ridge growth is less than the absolute growth rate because barb ridges grow helically around the circumference of the follicle. The angle of helical growth, θ, is also the angle at which a barb ridge intersects the rachis (Fig. 6, 7). If barb ridges have a constant diameter, then the horizontal component of barb growth, h, is a constant $m\sin(\theta)$, and the vertical component of growth, v, is $m\cos(\theta)$, or simply $v = \sqrt{m^2 - h^2}$ (Fig. 6). Thus, for the rachis, $v = m$ because $h = 0$. The horizontal and vertical components of growth are also affected by simultaneous growth in barb ridge diameter (see ***Barb ridge diameter***).

Initial barb number and new barb ridge addition function

Each feather begins growth with an initial number of barb ridges (Lucas and Stettenheim, '72) (Fig. 7). As they grow helically around the follicle, the barb ridges initially fuse to *form* the rachis, and then they subsequently fuse *to* the rachis. After fusion, the growth of a barb ridge ceases and the completed barb ridge is displaced upward and out of the follicle as the rachis grows at rate m (Fig. 6, 7). If the number of barb ridges in a feather was limited to the initial number, the vane of the feather would be quite restricted in size and shape. In order to have a substantial vane size and consequent complexity in shape, new barb ridges must form and be added to the follicle as the older barb ridges fuse to the rachis. Thus, the rate of new barb ridge addition is a critical parameter in determining feather shape.

The barb ridges in the follicle during feather growth can be modeled as a population of barb ridges whose contents over time is determined by analogous birth and death processes. The "birth" of barb ridges occurs through new barb ridge addition at the posterior new barb locus, and the "death" of barb ridges occurs as they fuse sequentially to the rachis anteriorly. The "population size" of the follicle at any moment determines the size of the follicle. Ultimately, the temporal "life span" and physical length of any barb ridge is de-

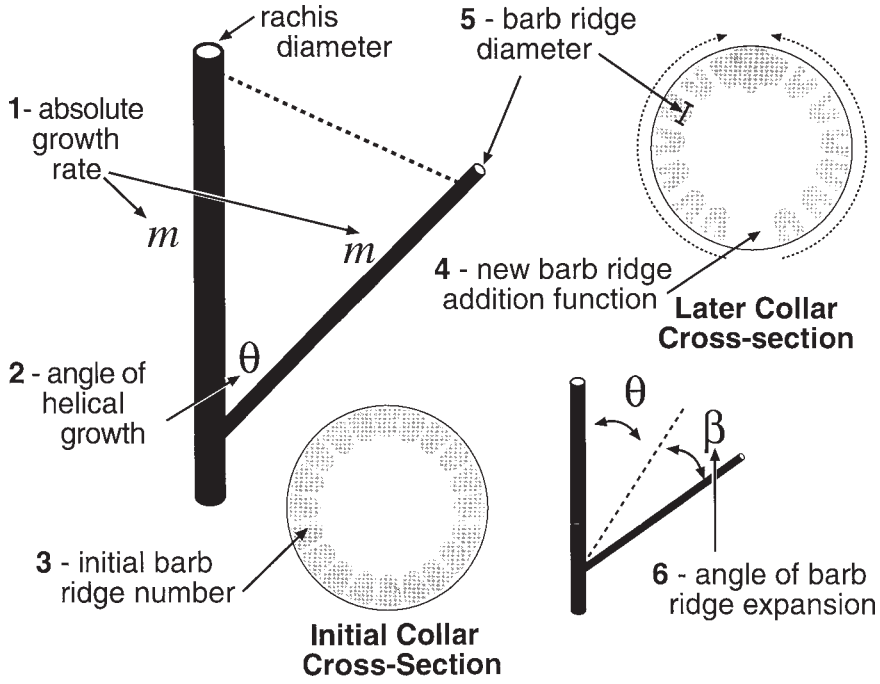

Fig. 7. Diagram of the six parameters of the model. 1: absolute growth rate, m. 2: angle of helical growth, θ. 3: initial barb ridge number. 4: new barb ridge addition function. 5: barb ridge diameter. 6: angle of barb ramus expansion after emergence from feather sheath, β.

termined by the growth rate and the follicle size. The rate of barb ridge fusion to the rachis, called D (for death), is determined by other parameters of the model:

$$D = \frac{m\sin(\theta)\cos(\theta)}{d_{\max}\Delta t} = \frac{h\cos(\theta)}{d_{\max}\Delta t} \quad (1)$$

where m is the absolute growth rate, θ is angle of helical growth, d_{max} is the maximum barb ridge diameter, Δt is the length of the minimum time increment in the simulation, and h is the horizontal component of barb ridge growth (with constant barb ridge diameter only). The fusion rate is maximized at $\theta = 45°$ and decreases at larger and smaller values of θ.

The addition of new barb ridges to the follicle is a distinct model parameter given by the function $B(t)$ (for birth) which gives the rate of barb ridge addition in units of new barb ridges added per unit time as a function of time. The model can accommodate almost any barb ridge addition function. In order to grow a substantial but finite vane length, however, the new barb ridge addition rate must start out greater than and end up less than the fusion rate D (eq. 1). Thus, the population of barb ridges in the collar must be greater than zero for the feather vane to continue to grow, and must be equal to zero for the feather vane to stop growing.

The simplest version of the new barb ridge addition function, $B_L(t)$, employed here is a linear decrease in barb ridge addition rate:

$$B_L(t) = -\frac{w}{t_{\max}}t + w + 1 \quad (2)$$

where t is time, t_{max} denotes the maximum time over which barbs are added, and w is the proportional deviation of the function from a constant value of one (Fig. 8A). The slope of the function can be varied by specifying different values of w. (One interesting advantage of this function is that the overall average rate of barb ridge addition remains constant for values of w between 0 and 1 despite the change in slope. For values of $w > 1$, the negative values of barb addition rate are defined as zero. Fig. 8A).

Alternatively, the rate of new barb ridge addition can be hypothesized as a decreasing linear function, B_{LD}, that is centered around (or with an average value between t_0 and t_{max} equal to) the barb ridge fusion rate, D:

$$B_{LD}(t) = -\frac{Dw}{t_{\max}}t + D(w+1) \quad (3)$$

With B_{LD}, the barb ridge addition rate is affected by the values of m, θ, and d_{max}.

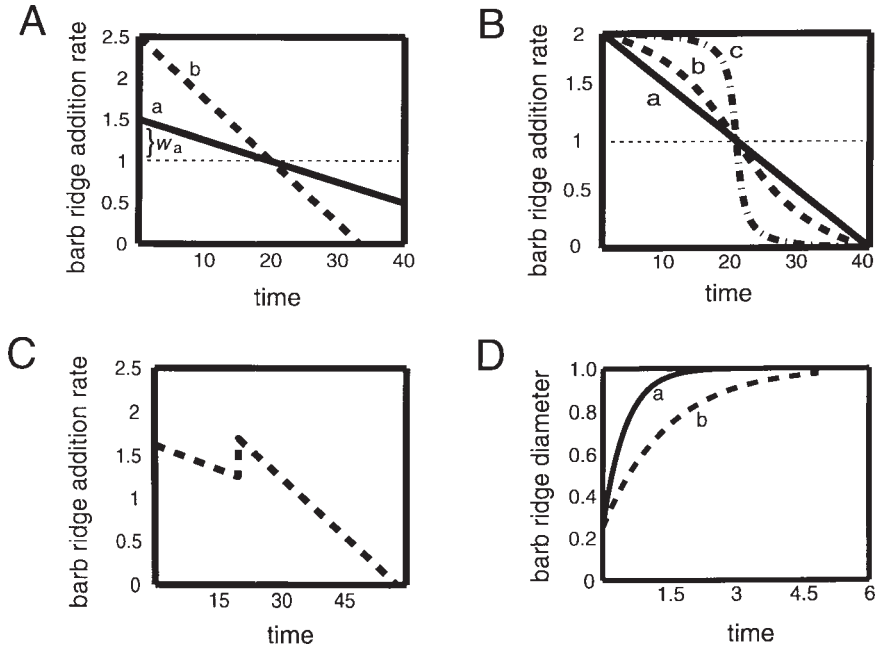

Fig. 8. Graphs of growth parameter functions. (**A**) Linear barb ridge addition function, B_L (eq. 2). Functions a and b differ in the value of w (a, w = 0.5; b, w = 1.5), the proportional deviation of the function from an average value of one (dotted horizontal line). An alternative fusion-rate centered barb ridge addition function, B_{LD} (eq. 3), has the same shape but is displaced vertically so that the horizontal constant equals the fusion rate, D (eq. 1). (**B**) Non-linear barb ridge addition functions, B_{NL} (eq. 4) . The function shape is determined by the variable q. At q approaches 0 (a, q = 0.001), the function approaches the linear function B_L. At intermediate values of q (b, q = 0.1), the function takes a sigmoidal shape centered on t_{max} /2. At large values of q (c, q = 1), the function approaches a step function centered at t_{max} /2. (**C**) Non-linear barb ridge addition function used in the simulation of the leading edge of the vane of an emarginate primary (Fig. 22). (**D**) Barb ridge diameter growth function (eq. 5). Shape of the function is determined by the variable α and the starting barb ridge diameter, d_0. At small values of α (a, α = 0.5, d_0 = 0.25, d_{max} = 1.0), the barb diameter rapidly approaches the maximum diameters, d_{max}. At larger values of α (b, α = 1.4, d_0 = 0.25, d_{max} = 1.0), the barb ridge diameter gradually approaches d_{max}.

We also employed a non-linear function, B_{NL}, chosen because it ranges from a linear function to a step function based on the value of a parameter q. It is written:

$$B_{NL}(t) = \frac{\arctan(-q(t - \frac{t_{\max}}{2}))}{\arctan(q\frac{t_{\max}}{2})} + 1 \quad (4)$$

where q is a parameter that determines the shape of the function (Fig. 8B). As q approaches 0, B_{NL} approaches the linear function B_L. As q becomes large, B_{NL} approaches a step function centered at $t_{max}/2$. For intermediate values of q, B_{NL} is an intermediate sigmoidal shape (Fig.8B).

Barb ridge diameter

In the feather follicle, barb ridges are typically elliptical in shape with the barbule plates extending toward the periphery and upward out of the follicle (Lucas and Stettenheim, '72). The width of the barb ridge determines how much each barb ridge contributes to the diameter of the follicle. In the model, we simplify the description of barb ridge size to the diameter of a cylinder (Fig. 7).

Growth in barb ridge diameter has complex effects on both the horizontal and vertical components of barb ridge growth. The barb closest to the rachis is always horizontally displaced at the rate $m\sin(\theta)$ (Fig. 9). If all barb ridges are equal in diameter (Fig. 9A), then all barb ridges grow with the same horizontal and vertical components of growth. But, if barb ridges grow in diameter as they grow in length, then both the angle of helical growth and the increase in barb diameter contribute to the horizontal component of barb ridge growth (Fig. 9B). Because barb ridges are constrained to grow adjacent to one another, the expansion in diameter of a barb ridge will constrain the horizontal component of growth of its posterior, neighboring barb ridge (Fig. 9B). Since the absolute growth in length of the barb ridges is

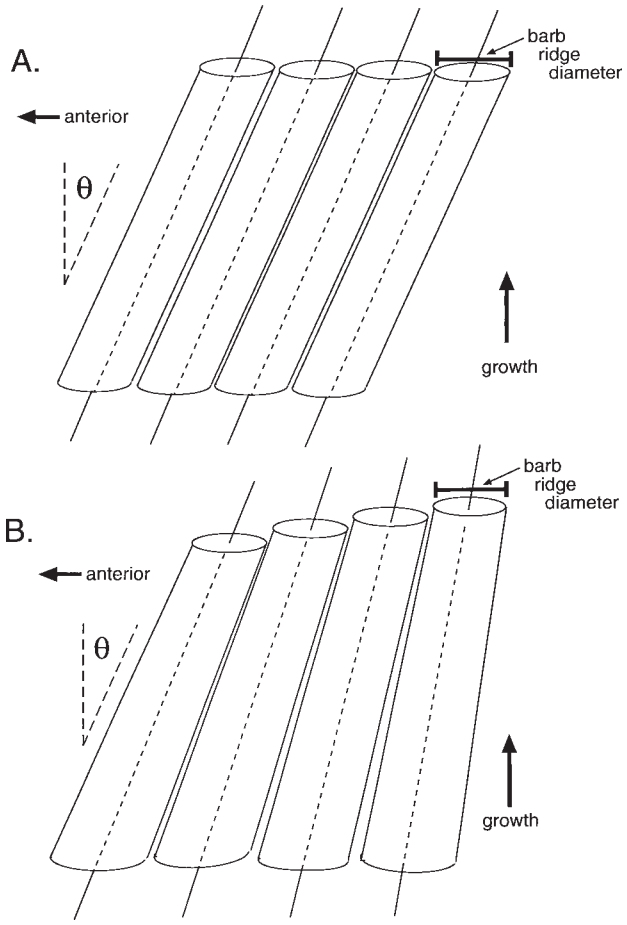

Fig. 9. The effect of growth in barb ridge radius on the horizontal component of growth. Each diagram depicts a series of adjacent barb ridges as if looking outward from inside the center of the follicle. The barbs are growing helically through time toward the anterior midline of the follicle at the left. (**A**) Barb ridges with constant barb ridge radius growing at an angle of helical growth, q. All barb ridges have uniform horizontal and vertical components of growth. (**B**) Barb ridges growing at the same angle of helical growth, θ (given by the anterior edge of the anteriormost barb ridge), but with simultaneous growth in barb ridge diameter do not have uniform horizontal and vertical components of growth. Because barb ridges are constrained to grow adjacent to one another, the horizontal component of growth of a ridge will be physically constrained by the growth in diameter of its anterior neighbor. Since the absolute growth in length of the barb ridges is uniform, a decrease in the horizontal component of growth of a barb ridge produces a compensating increase in its vertical component of growth. Uniform horizontal and vertical growth components are ultimately established among those barb ridges that have reached the maximum barb ridge diameter (d_{max}).

uniform, this decrease in the horizontal component of growth produces a compensating increase in the vertical component of growth. (Fig 9B). If $m^2 = h^2 + v^2$ and m is uniform throughout the follicle, then growth in barb ridge diameter will decrease h and compensatingly increase v until a barb ridge and its anterior neighbor have reached their maximum diameter. As a consequence of heterogeneous h and v, an isochrone will not form a straight chevron in the feather vane with simultaneous growth in length and diameter of barb ridges. Rather, in comparison to an isochrone from a feather with constant barb ridge diameter (Fig. 5), it will be curved toward horizontal at its lateral margins because of the increased vertical component of growth during the early stages growth in the younger, peripheral barb ridges (Fig. 10).

Barb ridge diameter can be assigned a constant

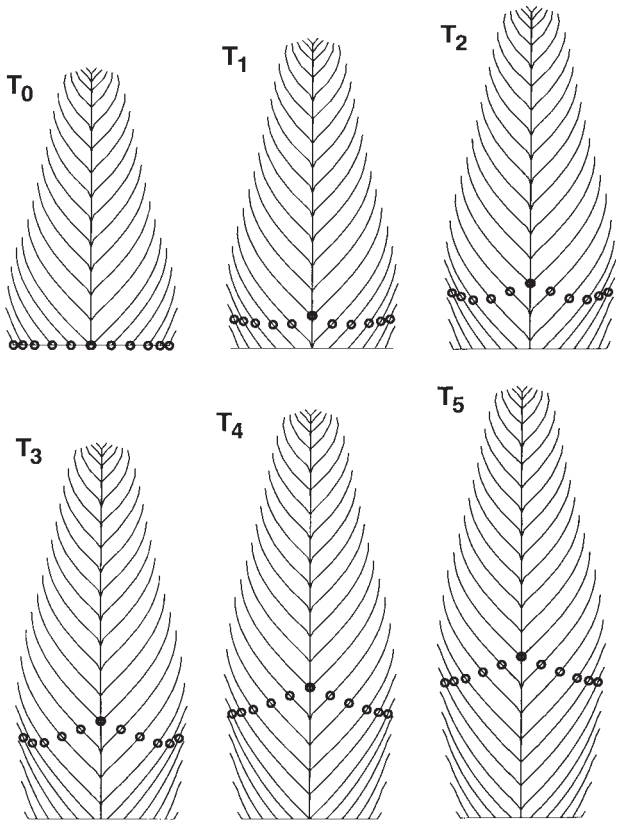

Fig. 10. The simulated spatiotemporal relationships among barb and rachis cells from an isochronic section of the follicle collar with simultaneous growth in the length and diameter of barb ridges depicted at six stages (T_0–T_5). (See Fig. 5 for general description). Because barb ridges are growing in diameter early in their development (Fig. 9B), the posterior points on the isochrone have initially larger vertical growth components and are displaced upward faster than the anterior points on the isochrone (T_1–T_4). Although vertical growth becomes uniform among barb ridges of maximum diameter, the more rapid initial vertical growth of the posterior portions of the isochrone is still observable in the laterally curved final shape of the isochrone (T_5).

value or modeled as function, $d(t)$, that exponentially approaches the maximum diameter d_{max} :

$$d(t) = d_{\max} - (d_{\max} - d_0)e^{-\frac{(t-t_0)}{\alpha}} \quad (5)$$

where t_0 is the time at which the barb formed, d_0 is the initial barb radius, d_{max} is the maximum diameter of a barb ridge, and α reflects the time it takes for the barb to reach the maximum diameter (Fig. 8D). As α decreases, the rate at which the barb approaches the maximum radius increases (Fig. 8D). The value of d_{max} was assumed to be constant during feather development. In feathers with constant ridge diameter, $d_0 = d_{max}$.

The rachis ridge is formed by the fusion of an initial pair of barb ridges early in feather growth at the anterior midline of the follicle (Lucas and Stettenheim, '72). Subsequent growth of the central medulla of the rachis ridge determines the diameter of the rachis (Fig. 7). A single simulation was conducted in which rachis ridge diameter growth was increased by a simple increment, *R,* for each barb ridge fused.

Angle of barb ramus expansion

As cell growth and keratinization proceed, the feather emerges from the follicle as a cylinder of branched filaments rolled up within a keratin sheath, commonly called a pinfeather. As the feather grows at its basal end, it begins to emerge from the sheath at its distal end. Emergence continues proximally until the entire sheath has fallen off. As they emerge from the sheath, the barb rami unfurl and expand outward to form the feather vane. At this time, the angle between the barb rami and the rachis expands so that the width of the emergent feather vane is larger than the diameter of the follicle (Fig. 7).

The angle of barb ramus shift, β, is modeled here as constant for the entire feather throughout its growth. For a symmetrical feather, the width of the vane, W, is given by:

$$W = (\sin\theta + \beta)(C\sin\theta) \quad (6)$$

where, θ is the angle of helical growth, β is the additional angle of barb ramus shift, and C is the circumference of the pin feather at that point, or sum of all the barb ridge diameters for the original horizontal cross-section.

The effect of the barb ramus expansion angle will be to widen the vane and create additional space between the barbs in the final emerged feather. The actual angle is likely determined by the size and the shape of the barb ramus cells which are determined during keratinization after cell proliferation in the collar.

Computational details

Our feather growth simulations begin with a specified number of barb ridges of a given radius and no rachis. Growth takes place in a series of time increments of length Δt during which each barb ridge present grows at the absolute growth rate m. In each time step, the diameter of each barb ridge is calculated, and the horizontal and vertical components of growth of each barb ridge are calculated, starting with the anteriormost barbs. The x and y coordinates of the center of each barb ridge are recorded in a matrix. These x and y values correspond to the position of the center of the barb ridge in the cylindrical collar during development, and also to the position of that barb in the planar vane of the feather after emergence (but prior to lateral barb expansion). At the end of each time step, any new barb ridges are added to the new barb locus on the posterior side of the follicle. When the first two barbs from the left and right side of the follicle meet at the anterior midline, they combine to form the rachis ridge. From this point on, the rachis grows vertically at rate m. When the center of a barb ridge intersects the margin of the rachis ridge, the barb is fused to the rachis and its growth ceases. After fusing to the rachis, barb ridges cease growing, but they are displaced upward at rate m with the rachis. Feathers continue to grow until all the barbs present in the follicle are fused to the rachis. Following the completion of cell growth, the barbs are shifted laterally, by an additional angle β, to simulate the expansion of the angle between the barb rami and the rachis. To create asymmetrical feathers, the model permits the independent specification of some parameter values for the left and right sides of the follicle.

All simulated feathers are illustrated with a standard scale bar. In all simulations, the number of barb ridges in the vane has been limited so that each barb is individually visible and the effects of the variables on shape are clear. Simulated feathers depict the barbs as simple lines down the center of the barb. For graphic convenience, barb diameter is not depicted with different line widths. In the one simulation with variable rachis diameter, however, the diameter of the rachis is depicted with differential line width. The position of bilateral or unilateral iso-

chronic fault bars was simulated by differentially plotting the set of cells produced during a specific time interval on the completed feather. A cross-section of the collar can also be simulated for any time step during feather growth by drawing a circle composed of the barb and rachis ridges of the appropriate size that are present in the follicle at that time. Variation in feather shape are described using standard botanical terminology for leaf shape. The mathematical model was constructed using MATLAB (Version 5) on a Macintosh G3 computer.

RESULTS

The model defines a theoretical, six-dimensional feather morphospace. The six growth parameter axes determine the theoretical feather shapes at each point in the morphospace. To explore this morphospace, we identified a set of intermediate growth parameter values that produced an idealized, standard elliptical feather shape (Fig. 11). These basic parameters include a constant growth rate (0.28), eight initial barb ridges (four on each side), a constant angle of helical displacement (θ = 45°), a decreasing linear barb ridge addition function (B_L, w = 1), constant barb ridge and rachis ridge diameters ($d_0 = d_{max} = 1$), no angle of barb ramus expansion (β = 0°), and identical parameter settings for both sides of the follicle. We then ran a series of simulations using more extreme values of each parameter independently, essentially exploring feather morphospace along six orthogonal parameter axes through the standard elliptical feather shape. Last, efforts were made to identify parameter values that simulate the complex shape of an emarginate or "notched" primary flight feather.

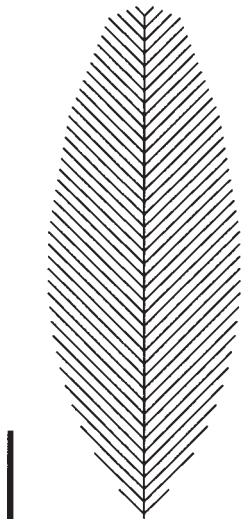

Fig. 11. The standard elliptical feather shape. Simulated under the following conditions: absolute growth rate, 0.28; angle of helical growth, 45°; initial barb ridge number, eight (four per side); linear decreasing barb ridge addition function B_L with w = 1; barb ridge and rachis ridge diameter constant at 1; angle of barb ridge expansion, 0°; time interval, 0.197.

Absolute growth rate

Differences in absolute growth rate, m, produce substantially different shapes of feather vanes (Fig. 12). A lower growth rate will produce a generally broader vane with a similar elliptical shape (Fig. 12A). A higher growth rate will result in a narrow vane, or lanceolate shape (Fig. 12C). The effect of differences in growth rate alone on shape is substantial because the new barb ridge addition function remains the same as in the standard elliptical feather (Fig. 11, 12B): a simple, linear decreasing function of time (Fig. 8A; eq. 2). A lower rate of growth means that barbs will take longer to reach the rachis and that the barb ridge fusion rate, D (eq. 1), will decline. However, the linear barb ridge addition function (eq. 2) will continue to add new barb ridges to the follicle at the same (though declining) rate over time as in the standard elliptical feather. The result of lower fusion rate and the same barb ridge addition function is: (1) an increase in the number of barb ridges in the follicle, (2) an increase in follicle diameter, (3) a consequent increase in the distances that barb ridges must grow to reach the rachis, and (4) the production of longer barbs and a wider vane. In contrast, a higher growth rate increases the barb ridge fusion rate, restricts the number

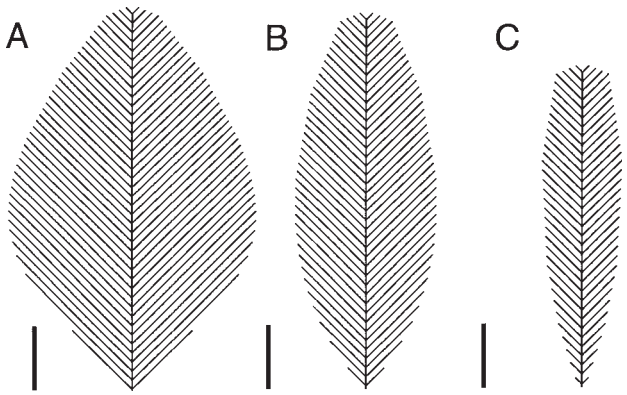

Fig. 12. Feathers simulated by varying the absolute growth rate. (**A**) Lower absolute growth rate, 0.18. (**B**) Standard growth rate, 0.28. (**C**) Higher growth rate, 0.38.

of barb ridges in the follicle and the diameter of the follicle, and creates a feather with shorter barbs and a narrower vane (Fig. 12C).

The predominance of the effects of growth rate on feather shape through the barb fusion rate can be shown by employing an alternative new barb ridge addition function, B_{LD} (eq. 3)—a declining, linear function centered around the fusion rate, D, which is proportional to the absolute growth rate. When the average of the new barb ridge addition function is adjusted by the growth rate, then changes in growth rate result in no change in feather shape (results identical to standard elliptical feather, fig. 11).

Angle of helical growth

Differences in angle of helical growth alone have complex effects on feather shape. Reducing the angle of helical growth, θ, produces a slightly longer vane with a slightly lanceolate shape (Fig. 13A). Increasing θ results in a longer and broader feather which is also broader at the base, or broadly ovate (Fig. 13C). Feathers with a smaller θ have longer narrower vanes with longer barbs (Fig. 13A) because a smaller θ decreases the horizontal component of growth and consequently increases the vertical component of growth. At smaller θ, barb ridges also approach the rachis more slowly per unit length, lowering the fusion rate (eq. 1). Thus, the barb ridges accumulate more length before they reach the rachis, fuse to it, and cease growing. In contrast, feathers with a larger θ have a broad vane of long barbs because the more oblique angle of barb ridge growth creates a larger follicle diameter for the same barb ridge diameter (i.e., a more oblique section of a barb ridge is wider than a more perpendicular section). The increase in follicle diameter increases the length barbs must grow in order to reach and fuse to the rachis.

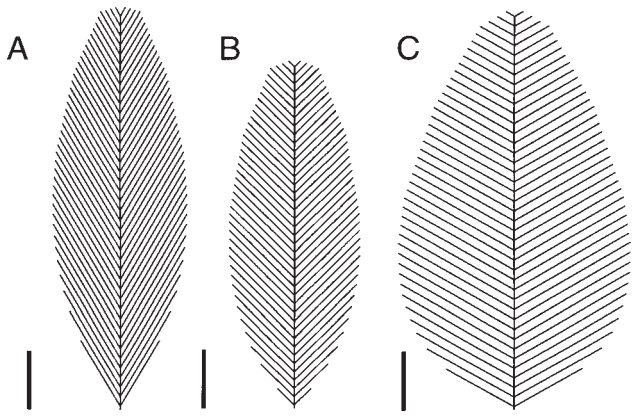

Fig. 13. Feather simulated by varying the angle of helical growth. (**A**) Smaller angle of helical growth, 30°. (**B**) Standard angle of helical growth, 45°. (**C**) Larger angle of helical growth, 60°.

Angle of helical growth also has complex effects on the internodal distance—the length of the rachis between fused barbs. The simulated feathers with both larger and smaller θ have larger internodal distances than the standard feather shape. This non-intuitive result can be understood by solving for the internodal distance. If the fusion rate, D, is:

$$D = \frac{m\sin(\theta)\cos(\theta)}{d_{\max}\Delta t} = \frac{m\sin(2\theta)}{2d_{\max}\Delta t} \quad (7)$$

then the internodal distance, ID, the distance between fusion events, is:

$$ID\frac{d_{\max}}{0.5\sin(2\theta)} \quad (8)$$

This function has a minimum at 45° (θ of the standard elliptical feather), and it increases exponentially with increasing or decreasing values of θ around 45°. Thus, the simulated feathers with larger and smaller values of θ had larger and identical internodal distances because the θ values were symmetrically divergent from the minimum of the internodal distance function, represented by the standard feather. Interestingly, internode distance is independent of the growth rate, m, and thus differences in growth rate alone do not produce differences in internodal distance (Fig. 12).

The angle of helical growth cannot increase during feather growth because barb ridges are constrained to stay next to one another within the cylindrical collar and a younger barb ridge cannot be horizontally displaced faster than its older, more anterior neighbor. The angle of helical displacement could theoretically increase during development of a feather, but the result would be barbs that converge on the rachis at successively larger internodal distances. Under these conditions, barbules of neighboring barbs would not likely interlock with one another to form a closed pennaceous vane (e.g., peacock tail plume).

Initial number of barb ridges

An increase in the initial number of barbs from 8 to 20 creates a feather that is broader, or obtuse, at its distal tip (Fig. 14A,B). The distal tip of the feather also shows more conspicuous "shoulders"—abrupt changes in the profile of the vane

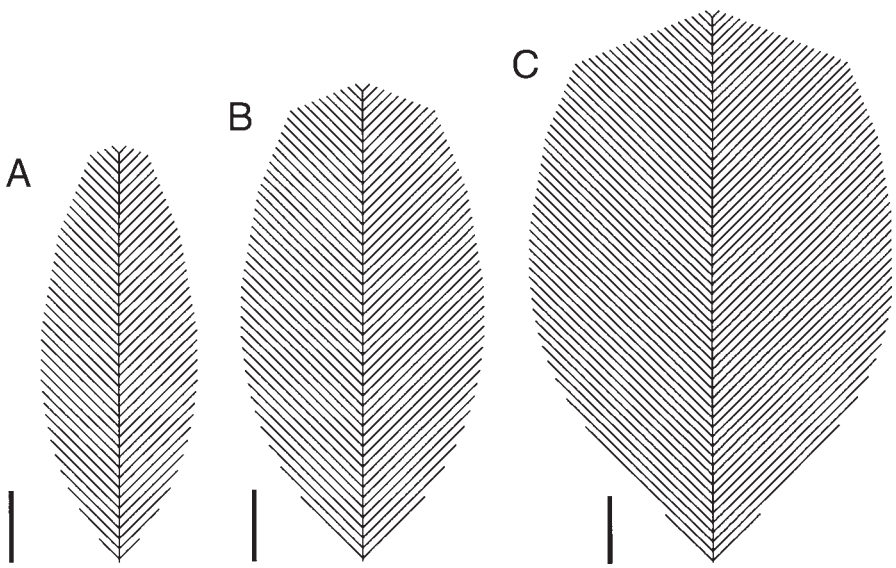

Fig. 14. Feathers simulated by varying the initial number of barb ridges. (**A**). Standard elliptical feather, initial barb ridge number, 8; (**B**) Larger initial barb ridge number, 20; (**C**) Very large initial barb ridge number, 40.

between the distal tips of the last of the initial barb ridges and the first new barb to be added to the follicle (Fig. 14B). A large increase in initial barb ridge number to 40 barbs produces a very broad tip and a wider vane that is cuneate in shape (Fig. 14C). Initial number of barb ridges contributes not only to the shape of the distal tip of the vane but to the length of the barbs and overall width of the vane because initial barb number also affects the size of the follicle.

New barb ridge addition function

The slope of the linear new barb ridge addition function (B_L—the rate of new barb ridge addition over time; eq. 2) is determined by the proportional deviation of the function from horizontal (w) (Fig. 8A). With smaller w (a more gradual slope), the shape of the feather changes from elliptical to a narrow linear shape (Fig. 15A). In contrast, for larger values of w (a steeper slope), the feather becomes broader in the center of the vane while remaining essentially elliptical in shape (Fig. 15C). Decreasing the slope of the barb ridge addition function does slightly reduce the total number of barb ridges in the feather vane. In this case, however, the overall average barb addition rate is constant, so the lower slope of the barb ridge addition function has a more profound effect on feather shape by limiting the number of barb ridges in the follicle at any one time, and, thus limiting the follicle diameter. Smaller follicle diameter reduces the amount of growth required for a barb ridge to reach the rachis, and so decreases the length of the barbs and the width of the vane. Likewise, an increase in the slope of the barb ridge addition function adds more barbs per unit time to the follicle early in its growth, produces a follicle with a larger diameter, increases the amount of growth required before fusion, and results in longer barbs and a broader vane.

Changes in the shape of the barb ridge addition function (Fig. 8B) produce substantial additional changes in feather shape (Fig. 16). A declining sigmoidal barb ridge addition function

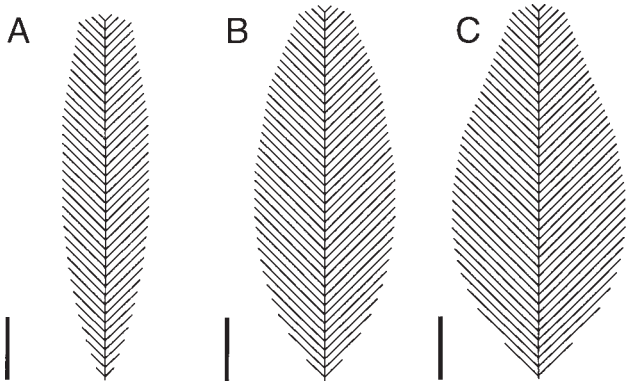

Fig. 15. Feathers simulated by varying the slope of the linear new barb ridge addition function (B_L, eq. 2; Fig. 8A). (**A**) Barb ridge addition function with shallower slope, w = 0.5; (**B**) Standard elliptical feather, w = 1. (**C**). Barb ridge addition function with steeper slope, w = 1.5.

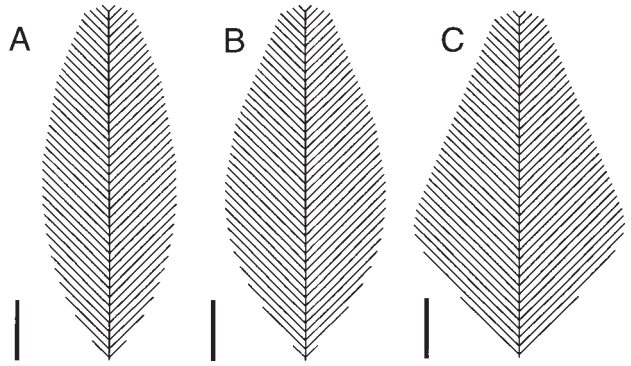

Fig. 16. Feathers simulated by varying the shape of the non-linear new barb ridge addition function (B_{NL}, eq. 4; Fig. 8B). (**A**) Standard elliptical feather with linear decreasing barb ridge addition function, q = .001. (**B**) Sigmoidal barb ridge addition function, q = 0.1. (**C**) Barb ridge addition step-function, q = 1.

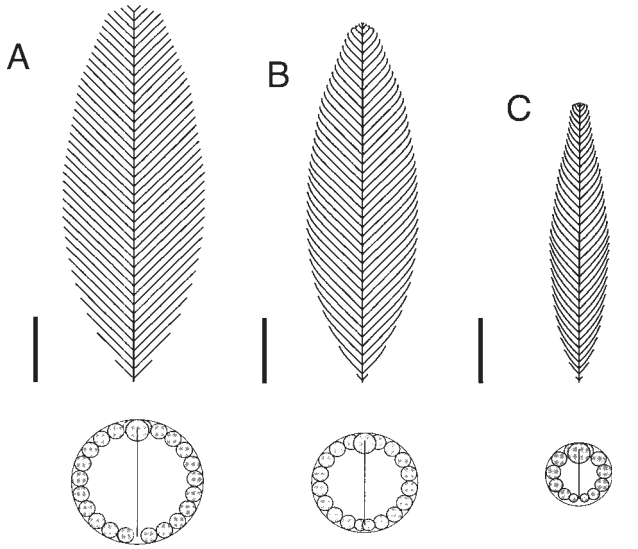

Fig. 17. Feathers simulated by varying the barb ridge diameter growth function (eq. 5; Fig. 8D). (**A**) Standard elliptical feather, $d_0 = d_{max} = 1.0$. (**B**) Feather with rapid growth toward maximum barb ridge diameter, $a = 0.5$, $d_0 = 0.25$, $d_{max} = 1.0$. (**C**) Feather with slow growth toward maximum barb ridge diameter, $a = 1.4$, $d_0 = 0.25$, $d_{max} = 1.0$. Below each feather is a simulated cross-section of the follicle at time stage 20 depicting the diameters of the barb ridges as they grow from the posterior (bottom) to anterior (top) surfaces of the follicle.

(B_{NL}; eq. 4, intermediate values of q) creates a significant widening in the middle of the vane but a maintenance of the generally elliptical shape (Fig. 16B). A nearly complete step function (high q values) creates a feather with a substantially wider vane toward its base, or strongly ovate shape (Fig. 16C). Given that each of these barb addition functions has the same average barb ridge addition rate, the consequent differences in shape are due the changes in the timing (or slope) of barb addition. The ovate feather shape produced by the sigmoidal barb ridge addition function (Fig. 16C) demonstrates that adding many barb ridges early in development produces a persistently larger follicle diameter which affects the lengths of many subsequent barb ridges. The result is a displacement in position of the widest point in the vane toward the base of the feather.

Barb and rachis ridge diameter

Barb ridge diameter affects the horizontal and vertical components of barb ridge growth, the distance between the barbs in the follicle, and thus the diameter of the follicle (Fig. 9). Feathers with an increasing diameter during barb ridge growth differ from those with constant barb ridge diameter in that barbs are curved at their tips toward the distal tip of the feather (Fig. 17B, C). This distal curve occurs because: (1) the horizontal component of growth is physically constrained in the follicle by the growth in diameter of the anterior-neighboring barb ridges, and (2) the vertical component of growth is compensatingly increased to maintain a constant absolute growth in length (Fig.9B).

The time required to grow to the maximum barb ridge diameter, α, also has a substantial additional effect on feather shape. A rapid approach to the maximum diameter, small α (Fig. 8D), produces a feather that is slightly narrower distally and broader in the basal half, or slightly ovate in shape (Fig. 17B). A gradual increase in barb radius, large α, produces a feather that is thinner, substantially shorter, and distinctly ovate in shape (Fig. 17C). These changes in shape are produced both by the curving barb tips, and by the short barb lengths which are a consequence of the limitations on follicle diameter from the smaller barb ridge diameters.

In addition, simulations of a linearly increasing rachis ridge diameter were conducted. The results were a realistic rachis (Fig. 18). However, the diameter rachis does not change the shape of the outline of the feather vane.

Angle of barb expansion

The angle of expansion of barb rami as the planar emerges from the cylindrical feather sheath widens the feather vane without changing the length of barbs (a necessary indirect effect of changing the angle of helical growth). For a given

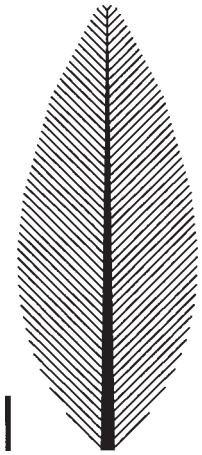

Fig. 18. Feather simulated with an incremental increase in the diameter of the rachis ridge, R, for every barb ridge fused. Rachis $d_0 = 1.0$.

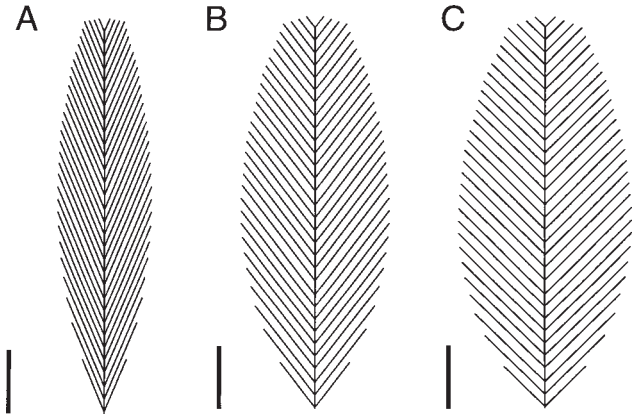

Fig. 19. Feathers simulated by varying the angle of barb ramus expansion, β, following emergence from the feather sheath, or pin feather. (**A**) Feather with no additional angle of barb expansion, $\theta = 22.5°$, $\beta = 0°$. (**B**) Feather with some additional angle of barb expansion, $\theta = 22.5°$, $\beta = 15°$. (**C**) Feather with large additional angle of barb expansion, $\theta = 22.5°$, $\beta = 22.5°$.

angle of helical growth, increasing angles of barb expansion will progressively widen the vane (Fig. 19). Furthermore, feathers with a constant sum of angles of helical growth and barb expansion ($\theta + \beta$) do not have the same shape. For example, four feathers with a sum of both angles equal to 45°, but varying in θ from 15–45°, vary extensively in vane width, internode distance, and length (Fig. 20). For a given total angle, a greater angle of barb expansion will increase the internodal distance, the width, and the total length of the feather but decrease the number of total barbs (Fig. 20A). Both parameters ultimately affect the angle at which barbs intersect the rachis, but angle of helical growth has additional complex effects on shape. Thus, both parameters are required to describe accurately the growth of feather shape.

Asymmetrical parameter settings

Asymmetrical feathers were generated by assigning different values for the initial barb number, barb ridge addition function, and barb ridge diameter function for the left and right sides of the feather follicle. A combination of lateral differences in the initial barb ridge number, and the

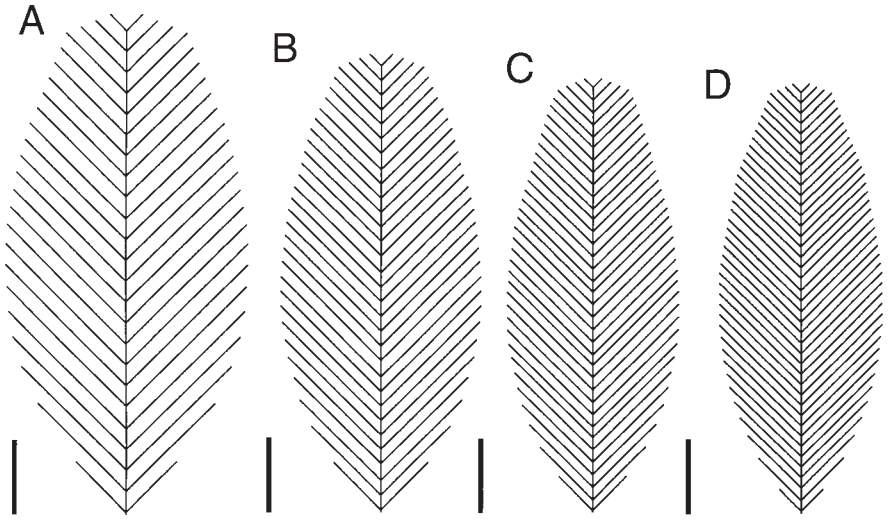

Fig. 20. Feathers simulated with a variable angle of helical growth (θ) and constant total angle of helical growth and barb expansion ($\theta + \beta = 45°$). (**A**) $\theta = 15°$, $\beta = 30°$. (**B**) $\theta = 22.5°$, $\beta = 22.5°$. (**C**) $\theta = 22.5°$, $\beta = 0°$. (**D**) Standard elliptical feather, $\theta = 45°$, $\beta = 0$.

slope of the linear barb ridge addition function (determined by w), with a laterally uniform angle of displacement and barb radius function will produce an asymmetrical feather with a narrower vane on one side (Fig. 21A,C). Lateral differences in the barb ridge addition function will produce differential increases in the number of barb ridges on each side of the follicle, differential growth in barb ridge population, and differences in size between the left and right sides of the follicle. Consequently, the two "sides" of the follicle will contribute differentially to the diameter of the follicle, and lead to the lateral displacement of the new barb locus within the collar toward the narrower side of the follicle (Fig. 21B,D). The lateral asymmetry in follicle size creates barbs of substantially different sizes on either side of the vane even though the number of barbs in each side of the vane is nearly identical (Fig. 21B).

We also explored an appropriate set of parameter values to simulate the growth of a specific type of asymmetrical feather: the emarginate, or "notched," primary in which the narrower vane of the leading edge of the primary narrows dramatically at the distal end of the feather. A nonlinear barb ridge addition rate function with an abrupt increase in the barb ridge addition rate at an intermediate time (Fig. 8C) will produce a feather with a widening in the middle of the vane (Fig. 22) that is typical of an emarginate primary feather.

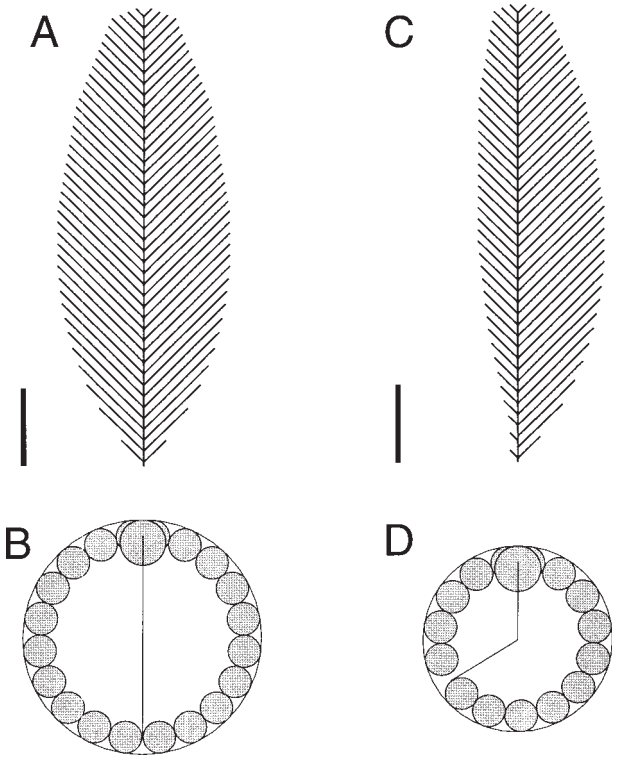

Fig. 21. Feathers simulated using symmetrical and asymmetrical parameter values. (**A**) Standard elliptical feather, all parameter values symmetrical. (**B**) Simulated cross-section of the follicle collar of the standard elliptical feather at time stage 12 showing the symmetrical positions of the anterior rachis ridge (top) and the posterior new barb locus (bottom). (**C**) Asymmetrical feather with fewer initial barb ridges (3) and a shallower linear barb ridge addition function (w = 0.4) for the left side, and the standard parameter values for the right side of the vane (initial barb ridge number = 4, w = 1). (**D**) Simulated cross-section of the follicle collar of this asymmetrical feather at time stage 12 showing the asymmetrical position of the new barb locus (lower left side) relative to the anterior rachis ridge (top). The differential initial barb ridge number and barb ridge addition rates for to the two sides of the follicle results in the faster growth of one side of the follicle and lateral displacement of the new barb locus.

Fig. 22. A simulated emarginate primary feather. The leading edge, or left side, of the feather vane was simulated with a special new barb ridge addition function with an intermediate jump in rate (w_{left} = 0.3; Fig. 8C), and the right side was simulated with the standard B_L with w_{right} = 1. All other parameters were symmetrical: growth rate, 0.28; d_{max} = 0.8; d_0 = 0.25; α = 0.8; angle of helical growth, 30°; initial number of barb ridges, 10 (5 per side); angle of barb expansion = 0°; time interval = 0.14.

In contrast to initial barb number, barb ridge addition rate, and barb diameter, the absolute growth rate and the angle of helical displacement apparently cannot be specified independently on the left and right sides of avian feather follicles. As argued previously, absolute growth rate is uniform throughout the collar. Although it is theoretically possible to have laterally different angles of helical growth, we know of no feathers that have this morphology.

Simulated isochronic fault bars

The position of isochronic fault bars were simulated on feathers by distinctly plotting the locus of cells that originated in a single time interval during growth (Figs. 5, 10, 23). The simulated fault bars show the same position observed in real feathers. For a feather with constant barb ridge diameter, fault bars are not at right angles to the rachis (Hardesty, '33), or at right angles to the barb rami ('Espinasse, '39), but form an isosceles triangle with the rachis and the barbs (Figs. 23A). The two equal sides of the isochronic isosceles triangle constitute the same amount of growth in the length of the barb and the rachis ridges from the time of origin in the collar until fusion (Fig. 6). With no additional angle of barb expansion, the two equal distal angles between the isochrone, the rachis, and the barbs equal $(180–\theta)/2$. Thus, the angle of deviation of the isochrone from horizontal is $90–((180–\theta)/2)$. Simultaneous growth in the diameter and length of the barb ridges creates a distal curve to the distal tips of the barbs (Fig. 10, 17), and results in a curved fault bar that is flattened out or upturned at the lateral margins of the vane (Fig. 23B).

The additional angle of barb ridge expansion will widen the vane and further displace the angle of the fault bar from near horizontal to a more prominent chevron-shape (Fig. 23C,D). The predicted angles of the fault bar to the rachis and barbs are given by the same expressions as above but with $(\theta + \beta)$ substituted for θ.

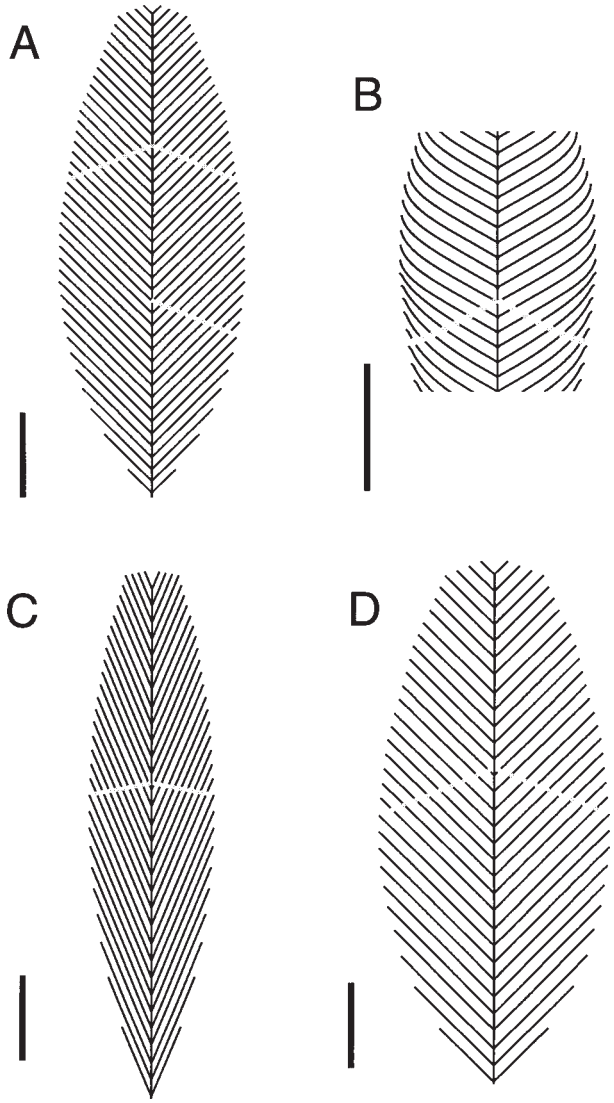

Fig. 23. Simulated fault bars. (**A**) Bilateral (above) and unilateral (below) fault bars simulated on the standard elliptical feather. (**B**). Detail of a unilateral fault bar simulated on a feather with simultaneous growth in barb ridge length and diameter (α = 0.5, d_0 = 0.25, d_{max} = 1.0.). Fault bar is curved toward horizontal at its lateral margins. (**C**) Bilateral fault bar simulated on a feather with an angle of helical growth, θ = 22.5°, and angle of barb ridge expansion, β = 0°. (**D**) Bilateral fault bar simulated on a feather with the same angle of helical growth as C, θ = 22.5°, but with a substantial additional angle of barb expansion, β = 22.5°.

DISCUSSION

The proposed mathematical model provides the first explicit theory of the growth of feather shape. Previously hypothesized mechanisms of feather shape determination have all been inexplicit, incomplete, or inaccurate (Lillie and Juhn, '32; 'Espinasse, '39; Lucas and Stettenheim, '72; Bleiweiss, '87). However, previous authors have proposed important parameters that were incorporated into this model: new barb ridge addition rate (Lucas and Stettenheim, '72), angle of helical growth of barb ridges (Bleiweiss, '87), and angle of barb expansion after emergence ('Espinasse, '39). The three additional parameters of our model—absolute growth rate, initial barb ridge number, and barb ridge diameter—are apparently proposed here for the first time.

We identified a set of parameter values that pro-

duce an idealized, standard, elliptical feather shape. We then varied the six parameters independently to explore the feather shape morphospace along the six orthogonal parameter axes through the standard feather shape. Avian contour feathers encompass many variations on elliptical shape, including those broadened basally into an ovate shape, those with a narrow linear tip with an ovate base (e.g., the hackle feathers of a chicken, *Gallus gallus*) or those with a broad tip gradually narrowing at the base (e.g., the breast feather of a turkey, *Meleagris gallipavo*). In contrast, avian remiges and rectrices (i.e., flight feathers) are characterized by variation in vane asymmetry, tip shape, length, and vane width. Most of our simulated feathers were purposefully simple (i.e., few barbs) so that the effects of growth parameters could be easily seen on barb length and vane shape. Nevertheless, the feather shapes simulated with this simple exploration of the morphospace encompass many of the variations in shape that characterize avian feathers. Furthermore, our single attempt to simulate a complex, realistic feather shape—the emarginate primary (Fig. 22)—reinforces the efficacy of the model. The model appears to be successful at simulating most feather vane shapes. Even some aspects of the simulated feather shapes that may appear to be computational artifacts at first are actually real features of feather shapes. For example, many simulated feathers have conspicuous "shoulders" on the distal margins of the vane between the tips of the last of the initial barb ridges and the first of the barbs to be added to the follicle. However, such "shoulders" are a prominent feature of many blunt-tipped contour feathers (which have a relatively large initial number of barb ridges). Furthermore, "shoulders" are not a necessary product of the model since some simulations identified parameter combinations that eliminated this feature of feather shape entirely (e.g., Fig. 17B, 18, 22). Comparison between simulated and real feathers confirms the efficacy of the model and establishes many explicitly testable predictions about the growth of feathers of different shapes.

Dynamics of the development of feather shape

Examining the effects of the various growth parameters on simulated feather shape supports a number of general conclusions about the developmental dynamics of the growth of feather shape. First, theoretically, all six parameters can have substantial independent effects on feather shape, and are potentially critical to shape specification during development.

Second, most parameters have complex, multiple effects on feather shape. For example, the barb ridge addition function can affect feather shape by influencing the total number of barbs in the vane. However, even if the average rate of barb addition is held constant (e.g., Fig. 15A, B; Fig. 16), differences in the slope of the new barb ridge addition function alone can have substantial effects on feather shape through follicle diameter. Similarly, barb ridge diameter growth produces curved barb tips, but it also limits follicle diameter and, therefore, barb length and vane width. The angle of helical displacement simultaneously affects barb length, follicle diameter, and the internodal distance. The model also predicts that the elliptical nature of many feather shapes—shorter barbs at the distal and basal ends with longer barbs in the middle—is a consequence of the fact that most barb ridge addition functions that will maintain a significant vane size with also produce an intermediate increase in follicle size and result in intermediate barbs with longer lengths.

Third, these parameters have many redundant effects on feather shape: many different parameter value combinations will create similar feather shapes. For example, either a higher growth rate (Fig. 12C) or a shallower slope on the linear barb ridge addition function (Fig. 15A) will produce nearly identical, shorter, linear feather shapes. Thus, many volumes of the six-dimensional feather morphospace describe feathers with identical shapes. In contrast, some parameters have unique effects on feather shape. For example, growth in barb ridge diameter produces a distal curving of barbs that is unique to this parameter.

Fourth, the complex and frequently redundant, multiple effects of each parameter create a system with complex developmental dynamics. For example, the absolute growth rate and the angle of helical growth both affect the fusion rate (eq. 1) which influences the diameter of the follicle, and thus barb length, vane width, and feather length. The barb ridge addition rate, the initial number of barbs, the angle of helical growth, and barb diameter growth all have independent effects on follicle diameter with similar important consequences for barb length, vane width, and feather shape. The horizontal and vertical components of barb ridge growth are determined by the growth

rate and angle of helical growth, but they can also be perturbed by simultaneous growth in barb ridge diameter. The internode distance is determined by barb ridge diameter and angle of helical growth but is independent of growth rate.

These six growth parameters form a complex causal nexus that likely determines feather shape. The interactions among parameters create a developmental system that is likely to be sensitive to fine developmental regulation and capable of creating exceptional diversity in form. Documenting shape variation along the parameter axes through a standard feather shape, as we have done here, is insufficient to describe all of the interactions among the parameters and their effects on feather shape. A thorough examination of many combinations of different parameter values will reveal more of the dynamics of feather shape growth. Explicit numerical analysis of the interrelationships of growth parameters could also be used to map completely the morphospace of pennaceous feather shape.

The model indicates additional aspects of feather morphology that must be correlated with these feather shape parameters in order to maintain feather function. In order to have a closed, pennaceous vane, the distal and proximal barbules must be long enough to effectively interlock across the space between adjacent barb rami. In the mature feather, the distance between parallel barb rami (*IB,* interbarb distance) is a function of the internodal distance (*ID* ; eq. 7), the angle of helical growth θ, and the angle of barb ridge expansion β:

$$IB = (ID)\sin(\theta + \beta). \tag{9}$$

Thus, to maintain a closed pennaceous vane of interlocking barbules, barbule length and morphology must be strictly correlated with both the angles of helical growth and barb ramus expansion.

The model predicts that feather asymmetries are determined by the independent specification of certain growth parameters for the left and right sides of the follicle. Asymmetries in the width of the vane appear to be a consequence of differential rates of barb ridge addition to the two sides of the follicle at the new barb locus. This process produces differential growth in the size of the two sides of the follicle, and results in the lateral displacement of the new barb locus from the posterior midline of the follicle toward the side of the feather follicle with the shorter vane (Fig. 21B,D). Our simulated result is confirmed by histological cross-sections of developing asymmetrical primary feather follicles that show the predicted lateral displacement of the new barb locus (Strong, '02; Hosker, '36; 'Espinasse, '39; Lucas and Stettenheim, '72). These simulations also predict that the classically emarginate primary—characterized by narrower leading-edge vane at the distal tip (Fig. 22)—is created by a nonlinear new barb ridge addition function with a sudden increase barb ridge addition rate in the leading edge side of the follicle during feather development (Fig. 8C).

Based on current results, however, it is simple to predict parameter value combinations that could generate many other derived feather shapes including afterfeathers, filoplumes, plumulaceous downs, spatulate or racket-tipped feathers (e.g., Bleiweiss, '87), and other specialized display plumes. These simulations will be the subject of future research.

Realism of the model

Although congruence between the shapes of simulated feathers and real feathers can confirm the efficacy of our model, it cannot be used by itself to support its realism. The ability of any theoretical or mathematical model to mimic a natural form must be challenged by detailed observations of the natural phenomenon being modeled before one can conclude that the intellectual model has any bearing on natural process (e.g., Niklas, '94). Thus, it is important to scrutinize the parameters of the model and compare them to the known details of how feathers grow.

It is clear that a classical allometric analysis—e.g., describing the distortions to a grid superimposed on different feather shapes (Thompson, '42)—would not be an appropriate model of feather shape determination because the parameters of a purely allometric analysis do not apply to the follicular mechanisms by which feathers grow. In contrast, the proposed theory and mathematical model are based on parameters that, with one exception (i.e., absolute growth rate; see discussion later in this article), are previously recognized to be occurring during feather growth (Lucas and Stettenheim, '72). Thus, all feathers start development with an initial number of feather barb ridges. In the absence of an aftershaft, new feather barbs are added to the follicle at the posterior new barb locus (Lucas and Stettenheim, '72). Barb ridges are known to grow helically to form and to fuse to the rachis at the anterior midline of the follicle (Lucas and Stettenheim, '72). It is directly observable that different feathers differ in the

angle at which barbs fuse to the rachis. (Mature plumulaceous barbules are less rigid and can assume many angles to the rachis, obscuring the angle of helical growth during their development.) It is also observable that the width of a pennaceous feather's vane is greater that the circumference of the pin feather, and that, therefore, there must be some additional angle of expansion by the barbs after emergence from the sheath (S. Gatesy, personal communication). It is also observable that barb ridges vary in diameter. In those feathers where barb diameter increases gradually, the barbs display a characteristic curve toward the distal tip of the feather at their distal ends, as predicted by the model. The model's ability to generate similar feathers is not by itself convincing, but the observation that these distortions in shape occur under the same conditions in simulated feathers as observed in real feathers indicates that the model constitutes a realistic and accurate theory of feather growth.

One growth parameter in the model—uniform absolute growth rate—has not been previously recognized as a feature of feather development. Solid evidence of a uniform barb and rachis ridge growth rate has been available since Fraps and Juhn ('36a), but it is apparent that Fraps and Juhn ('36a) and other subsequent researchers (Lillie and Juhn, '38; 'Espinasse, '39; Lillie, '40, '42; Lillie and Wang, '40; Lucas and Stettenheim, '72) interpreted these data as supporting uniform *axial* growth rates. Based on our interpretation of these data, we propose that *absolute* growth rates are uniform throughout the follicle, and that the *axial* growth rates of the barbs and rachis differ from one another accordingly (Fig. 6). This fundamental feature of the helical growth of feather barb ridges has a profound effect on the shape of feathers and the spatiotemporal composition of the pennaceous feather vane (Figs. 5, 10). As a consequence of uniform growth rates, helical growth, and the additional angle of barb expansion, an isochronic section of a feather is distorted during growth from horizontal at inception in the collar to an oblique chevron in the mature feather (Figs. 5, 10, 23). It is not generally appreciated that a horizontal section of a feather vane is not isochronic. For example, horizontal isochrones were depicted in an important illustration in Lucas and Stettenheim ('72: 370, Fig. 236) that has been widely reproduced in other publications. We have further established that simultaneous growth in the length and diameter of barb ridges creates additional heterogeneity in the horizontal and vertical components of growth among barb ridges of different diameters, and that the "conservation" of growth rate has additional effects on the shape of an isochrone and the entire feather vane (Fig. 10, 17, 23B). The experimental simulation of fault bars with the same oblique chevron position observed in real feathers is a strong confirmation of the uniform absolute growth rate hypothesis and further supports the realism of the model.

Except for diel variations (Lucas and Stettenheim, '72), the model's assumption of constant uniform absolute growth rates appears to be upheld by a number of studies of the growth in length of pin feathers (Lillie and Juhn, '32, '38; Lillie, '40; Lillie and Wang, '41). Interestingly, Lillie and Juhn ('32) observed that pin feather length grows at an initially slow and constant rate until the rachis is formed, after which it suddenly grows at a second, much faster rate. Given our new interpretation of the growth rates of barb and rachis ridges, we predict that these "two phases" of growth correspond to different components of a single absolute growth rate. Prior to the formation of the rachis, the length of the feather grows only at the rate of the vertical component of barb ridge growth: $v = m\cos(\theta)$. After the rachis is formed, feather length grows at the vertical growth of the rachis, which is equal to the absolute growth rate, m, of the follicle. Thus, we would predict that the differences between the rates of growth in length of the developing feather during these "two phases" varies according to the angle of helical growth of the barb ridges in the follicle.

Five of the six proposed model parameters are limited to simulating growth by cell division. Additional growth by increase in cell size and changes in cell shape continues to occur during keratinization in the barb ridges and the rachis ridge for some time after cell division in the collar (Lucas and Stettenheim, '72). Differential growth in cell size and shape has profound effect on feather morphology (e.g., distal and proximal barbule differentiation that creates the closed pennaceous vane, Fig. 1B) and various aspects of feather shape. For example, the rachis of many feathers is curved or distorted in shape from perfectly straight. Furthermore, the vane of many feathers is not planar, as assumed in the model, but curved. These shape changes are hypothesized to be produced by differences in cell size and shape which develop in the keratinocytes of the rachis, barbs, and barbules after cell division in the collar.

Tests of the model

The first important test of the model would be to document values of the proposed growth parameters during development from pennaceous feathers of different shapes. These parameters could be estimated by pooling samples of feather germs of different ages from the same shape class, or some parameters may be estimated from 3D reconstructions of serial histological sections of feather germs. Average values of some of these parameters have been estimated for entire feathers (e.g., barb ridge addition rate; Hardesty, '33), but these estimates have not taken into account the fact that some parameters must vary during development. Variations in these parameters have rarely been explicitly associated with differences in feather shape, though Lillie and Juhn ('32) documented that the long, lanceolate hackle feathers of chickens grow at a slower rate than do the elliptical contour feathers.

Specific observations are required to examine whether feather shape varies as predicted with variation in the proposed growth parameters. More detailed observations are required to confirm whether absolute growth rates are stable over days during feather development, or whether angle of helical growth remains constant. Explicit observations are also necessary to confirm the general match in position between simulated isochrones and real fault bars, and to see whether fault bars vary in shape and position in feathers with substantial growth in barb ramus diameter. The new barb ridge addition functions used here are merely heuristic. Direct observations are required to document the actual function of barb ridge addition during the growth of differently shaped feathers.

The realism of the model parameters does not indicate what parameter values are actually involved in the growth of real bird feathers. Sophisticated tests of our model would identify which of the theoretically plausible parameter combinations actually occur during the growth of differently shaped feathers in different taxonomic groups of birds. Many different parameter combinations (i.e., volumes of the feather morphospace) may be represented throughout avian diversity, or there may be biases toward specific combinations of parameter values determining feather shapes (i.e., subspaces) within different taxonomic groups. There may also be absolute constraints against specific parameter value combinations in all birds. Constraints against specific parameter combinations that are morphologically redundant will not reflect natural selection on phenotype if the resulting feather shapes are actually identical. Rather, such parameter constraints will likely be due to genetic correlations among growth parameters, historical constraints from the evolution of feather shape, or fundamental physical limitations of the molecular or cellular mechanisms of feather growth that are currently unknown. Differences among parameters in lateral differentiability may reflect differences in the fundamental mechanisms by which these parameters are specified in the follicle. Theoretically, different parameters may be specified either in the follicle as a whole, in the left and right sides of the follicle, in the main vane and the afterfeather, within individual barb ridges, or within the ramus and the proximal and distal barbule plates of the barb ridge. Not all parameters can be independently specified in each partition of the collar, but some parameters must be independently specified in each to grow the diversity of feather shapes and structures. Last, the most advanced tests of the model could include experimental perturbations of feather development, breeding experiments focusing on the genetics of feather shape, and molecular developmental analyses of the cellular and molecular mechanisms of feather shape determination.

Feather development has long been a model system for the study of mesenchyme epithelium interactions (e.g., Sengel, '76), and recent molecular studies of feather development have begun to explore the molecular mechanisms that determine the position and early development of feathers (e.g., Chuong and Widelitz, '98). However, much remains to be learned about the developmental processes involved in the later stages of feather development during which the events that determine feather structure and shape take place. For example, experimental studies of the molecular mechanisms involved in the determination of the model's parameters would contribute to a unified understanding of the growth of feather shape.

Evolution of feather shape

As with the question of the origin of feathers themselves, studying the evolutionary origin of feather shape determination is constrained by the absence of obvious intermediate or plesiomorphic morphologies (Prum, '99). By the first appearance of the feathers of *Archaeopteryx* in the Upper Jurassic, avian follicles had already evolved the capacity to grow feathers of modern

diversity of sizes and shapes including symmetrical wing coverts, and asymmetrical remiges and rectrices (de Beer, '54). These earliest known follicles had already evolved all the parameters of the proposed model, and the ability to independently specify some of these parameters on either side of the feather follicle. Thus, it is impossible to address the evolutionary origin of the mechanisms of feather shape determination with an analysis of feather shape distribution in modern birds because all the relevant parameters and the general classes of feather shape are plesiomorphic to extant birds. Given the corroborated phylogenetic hypotheses supporting birds as a lineage of theropod dinosaurs (Gauthier, '86; Padian and Chiappe, '98; Sereno, '99) and the recent evidence of filamentous integumental filaments that may be homologous with feather (Chen et al., '98; Ji et al., '98; Xu et al., '99a,b), the origin of feather shape and its determination may lie within more basal lineages of non-avian theropod dinosaurs.

Recently, Prum ('99) proposed a developmental theory of feather origins that hypothesized a transition series of feather morphologies from the first hollow cylindrical feather to the modern closed pennaceous feather based on the details of feather development. This developmental model provides some predictions about the historical process of the evolution of feather shape determining growth parameters. For example, the model hypothesizes that the origin of barb ridges preceded the origin of helical barb ridge growth and the rachis. This hypothesis would imply that initial barb ridge number and barb ridge diameter evolved prior to the origin of the angle of helical growth and the new barb addition function. Further, even the most plesiomorphic, cylindrical feather morphology would have been characterized by some growth rate, implying that absolute growth rate was the first of the six parameters to evolve. Because of the complex interrelationship among the feather growth parameters, the historical sequence in which the parameters evolved may have created historical constraints on the evolution of feather shape determination. This possibility could be tested by comparing the theoretical biases in feather shape determination predicted by various sequences of parameter origin with the actual differences between the theoretical and the realized feather morphospaces.

Feather shape and the distribution of feather shapes over the body have continued to evolve and diversify since their origins within clades of modern birds. An important early (probably pre-avian) event in the evolution of feather shape would have been the decoupling of the developmental determination of shape of feathers on various parts of the body. Independent shape determination would have allowed the diversification of feather shapes over the body for different functions. The subsequent evolution of feather diversity can be viewed as a historical and phylogenetic exploration of the potential feather morphospace. This theory of the growth of feather shape provides a framework for mechanistic analyses of the evolution of the shape of pennaceous feathers within and among lineages of extant birds.

Given the correlation between the shapes and apparent functions of many feathers (Stettenheim, '76), variation in feather shape within extant avian clades provides opportunities to test hypotheses about adaptive differentiation and natural selection on feather morphology. Among the many potential, naturally selected feather functions are flight, thermal insulation, physical protection, water repellency, communication, camouflage, etc. (Stettenheim, '76). This model provides detailed predictions about the developmental changes required to evolve specific, functional feather shapes. For example, many aerodynamically important features of the wings —wing shape, area, loading, and aspect ratio—are at least partially determined by the shape and size of the remiges. Natural selection for changes in the aerodynamic properties of wing shape will necessarily select on the developmental parameters that operate within feather follicles to influence the shape of the remiges. Detailed comparative analyses of the growth of variations in remige shape that effect aerodynamic function will provide further insights into this relationship.

The historical process of the adaptive exploration of the feather morphospace by avian lineages may have created contingencies or other constraints on subsequent exploitation of the morphospace. As in any adaptive landscape, certain functionally superior phenotypes may be bounded by functionally inferior shapes. Depending on historical and genetic conditions, this may have prevented the exhaustive or thorough exploration of feather morphospace. Theoretical analyses of the evolution of vascular plant shape by Niklas ('97; '99) also document the importance of the historical sequence of different sources of natural selection on shape in affecting outcome of evolutionary processes. Documenting the realized feather morphospace of birds and its phylogenetic com-

ponents of variations will provide a rich new understanding of the history of feather evolution.

The diversity of ornamental feathers that function specifically in intraspecific communication provides opportunities to examine the effect of sexual selection (Andersson, '94) and other social selection (West-Eberhard, '79) on feather shape. Elaborate, highly derived feather shapes have evolved for intersexual signaling in many groups of polygynous birds (e.g., birds of paradise, Paradisaeidae; Frith and Beehler, '98). Ornamental feathers provide a less constrained perspective on the evolution of feather function since these feathers have largely been released from a primarily physical function to a primarily psychological function (i.e., fulfilling the preferences of potential mates). For example, long tail feathers have frequently been hypothesized to have evolved as secondary sexual signals of mate quality in birds (Andersson, '82, '94; Møller, '88, '89, '91) with little consideration of the developmental changes required to evolve such tail feathers (for an exception, see Bleiweiss, '87). Interestingly, elongate, ornamental tail feathers are often associated with extreme variation in shape, even within a single genus in which the elongate plumes are homologous (e.g., *Alectrurus, Vidua, Tanysiptera*). The model provides detailed theoretical predictions about why selection on tail length might also produce diverse changes in feather shape. If novel female preferences for longer, more conspicuous tail feathers act on available genetic variation for the different growth parameters that effect tail feather length (e.g., growth rate, barb ridge addition rate, angle of helical growth. etc.), then variation among populations or lineages in the genetic variation within, and genetic correlation among, these growth parameters would result in longer feathers in different populations based on distinctly different parameter combinations. Because of the complex interactions among growth parameters, the result would also be additional variation in the shape of the vanes of these elongate feathers. Thus, the complexity of feather shape determination mechanisms provide an inherent source of diversity of feather shape in response to selection.

ACKNOWLEDGMENTS

Special thanks to Michael Christianson for providing helpful, constructive, and enthusiastic insights into developmental biology. Alan Brush and Peter Stettenheim shared freely of their knowledge of feathers. The research also benefited from discussions with George Barrowclough, Kim Bostwick, Steven Gatesy, Matt Harris, Town Peterson, Mark Robbins, and Kristof Zyskowski. The manuscript was improved by comments from Alan Brush and an anonymous reviewer.

LITERATURE CITED

Andersson M. 1982. Female choice selects on extreme tail length in a widowbird. Nature 299:818–820.

Andersson M. 1994. Sexual selection. Princeton, NJ: Princeton University Press.

Ball P. 1998. The self-made tapestry: pattern formation in nature. Oxford: Oxford University Press.

Beebe WH. 1910. Racket formation in the tail-feathers of the motmots. Zoologica 1:140–149.

Bleiweiss R. 1987. Development and evolution of avian racket plumes: fine structure and serial homology of the wire. J Morphology 194:23–39.

Brush AH. 1993. The origin of feathers. In: Farner DS, King JS, Parkes KC, editors. Avian biology. London: Academic Press, p 121–162.

Brush AH. 1996. On the origin of feathers. J Evol Biol 9: 131–142.

Chen P-J, Dong ZM, Zhen SN. 1998. An exceptionally well-preserved theropod dinosaur from the Yixian formation of China. Nature 391:147–152.

Chuong C-M. 1993. The making of a feather: homeoproteins, retinoids, and adhesion molecules. BioEssays 15:513–521.

Chuong C-M, Widelitz RB. 1998. Feather morphogenesis: A model of the formation of epithelial appendages. In: Chuong C-M, editor. Molecular basis of epithelial appendage morphogenesis. Georgetown, TX: R.G. Landes, p 57–74.

Chuong C-M, Oliver G, Ting SA, Jegalian BG, Chen HM, De Robertis EM. 1990. Gradients of homeoproteins in developing feather buds. Development 110:1021–1030.

Davies HR. 1889. Die Entwicklung der Feder und ihre Beziehungen zu anderen Integumentgebilden. Morph Jahrb 15:560–645.

de Beer G. 1954. *Archaeopteryx lithographica*; a study based on the British Museum specimen. London: Trustees of the British Museum.

Dyck J. 1985. The evolution of feathers. Zoologica Scripta 14:137–153.

Edelman GM. 1988. Topobiology. New York: Basic Books.

'Espinasse PG. 1934. Bilateral gynandromorphism in feathers. Nature 133:330.

'Espinasse PG. 1939. The developmental anatomy of the Brown Leghorn breast feather, and its reactions to oestrone. Proc Zool Soc London 109:247–288.

Fraps RM, Juhn M. 1936a. Developmental analysis in plumage. II. Plumage configurations and the mechanism of feather development. Physiol Zool 9:319– 377.

Fraps RM, Juhn M. 1936b. Developmental analysis in plumage. III. Field functions in the breast tracts. Physiol Zool 9:378–408.

Frith CB, Beehler BM. 1998. The Birds of Paradise. Oxford: Oxford University Press.

Gauthier JA. 1986. Saurischian monophyly and the origin of birds. Mem California Acad Sci 8:1–55.

Greite W. 1934. Die Strukturbildung der Vogelfeder und ihre Pigmentierung durch Melanine. Zeit wiss Zool 145:284–334.

Hardesty M. 1933. The feather of guinea fowl and a mathematical theory of individual feather patterns. J Exper Zool 66:53–86.

Hosker A. 1936. Studies on the epidermal structures of birds. Phil Trans Royal Soc London, B 226:143–188.
Ji Q, Currie PJ, Norell MA, Ji S-A. 1998. Two feathered dinosaurs from northeastern China. Nature 393:753–761.
Juhn M, Fraps RM. 1936. Developmental analysis in plumage. The individual feather: methods. Physiol Zool 9:293–317.
Lillie FR. 1940. Physiology of development of the feather. III. Growth of the mesodermal consituents and blood circulation in the pulp. Physiol Zool 13:143–175.
Lillie FR. 1942. On the development of feathers. Biol Rev 17:247–266.
Lillie FR, Juhn M. 1932. The physiology of development of feathers. I. Growth-rate and pattern in individual feathers. Physiol Zool 5:124–184.
Lillie FR, Juhn M. 1938. Physiology of development of the feather. II. General principles of development with special reference to the after-feather. Physiol Zool 11:434–448.
Lillie FR, Wang H. 1940. Physiology of development of the feather. IV. The diurnal curve of growth in brown leghorn. Proc Nat Acad Sci 26:67–85.
Lillie FR, Wang H. 1941. Physiology of development of the feather. V. Experimental morphogenesis. Physiol Zool 14:103–133.
Lucas AM, Stettenheim PR. 1972. Avian anatomy–integument. Washington, DC: U.S. Department of Agriculture.
Møller A. 1989. Viability costs of male tail ornaments in a swallow. Nature 339:132– 135.
Møller A. 1991. Sexual selection in monogamous Barn Swallows. I. Determinants of tail ornament size. Evolution 45:1823–1836.
Møller AP. 1988. Female choice selects for male sexual tail ornaments in the monogamous swallow. Nature 332:640–642.
Niklas KJ. 1994. Simulation of organic shape: The roles of phenomenology and mechanism. J Morphology 219:243–246.
Niklas KJ. 1997. Adaptive walks through fitness landscapes for early vascular land plants. American J Botany 84:16–25.
Niklas KJ. 1999. Evolutionary walks through a land plant morphospace. J Exper Biol 50:39–52.
Nohno T, Kawakami Y, Ohuchi H, Fujiwara A, Yoshioka H, Noji S. 1995. Involvement of the *Sonic Hedgehog* gene in chick feather development. Biochem Biophys Res Com 206:33–39.
Padian K, Chiappe LM. 1998. The origin and early evolution of birds. Biol Rev 73:1–42.
Prum RO. 1999. Development and evolutionary origin of feathers. J Exp Zool (Mol Dev Evol) 285:291–306.
Raup D, Michelson A. 1965. Theoretical morphology of a coiled shell. Science 147:1294–1295.
Sawyer RH, Knapp LW, O'Guin WM. 1986. The skin of birds: epidermis, dermis, and appendages. In: Bereiter-Hahn J, Matoltsky AG, Richards KS, editors. Biology of the integument: 2 vertebrates. Berlin: Springer-Verlag, p 194–238.
Sengel P. 1976. Morphogenesis of skin. Cambridge: Cambridge University Press.
Sereno P. 1999. The evolution of dinosaurs. Science 284:2137–2147.
Spearman RIC. 1973. The integument. Cambridge: Cambridge University Press.
Stettenheim P. 1972. The integument of birds. In: Farner DS, King JR, editors. Avian Biology. New York: Academic Press, p 1–63.
Stettenheim P. 1976. Structural adaptation in feathers. Proc Internat Ornithol Congr 16:385–401.
Strong RM. 1902. The development of color in the definitive feather. Bull Mus Comp Zool 40:147–185.
Thompson DW. 1942. On growth and form. Cambridge: Cambridge University Press.
Ting-Berreth SA, Chuong C-M. 1996a. Local delivery of TGFβ2 can substitute for placode epithelium to induce mesenchymal condensation during skin appendage morphogenesis. Dev Biol 179:347–359.
Ting-Berreth SA, Chuong C-M. 1996b. *Sonic Hedgehog* in feather morphogenesis: Induction of mesenchymal condensation and association with cell death. Dev Dynamics 207:157–170.
Wagner HO. 1959. Observations of the racket-tips of the motmot's tail. Auk 67:387–389.
West-Eberhard MJ. 1979. Sexual selection, social competition, and evolution. Proc Amer Phil Soc 123:222–234.
Xu X, Tang Z-l, Wang X-l. 1999a. A therinzinosauroid dinosaur with integumentary structures from China. Nature 399:350–354.
Xu X, Wang X-l, Wu X-C. 1999b. A dromeosaurid dinosaur with a filamentous integument from the Yixian Formation of China. Nature 401:262–266.
Young MC. 1999. The Guinness book of records 1999. New York: Bantam Books.